NATIONAL ADVISORY COMMITTEE FOR AERONAUTICS

TECHNICAL NOTE 3498

EXPLORATORY INVESTIGATION OF AN AIRFOIL WITH AREA SUCTION APPLIED TO A POROUS, ROUND TRAILING EDGE FITTED WITH A LIFT-CONTROL VANE

By Robert E. Dannenberg and James A. Weiberg

Ames Aeronautical Laboratory
Moffett Field, Calif.

Washington
April 1955

NATIONAL ADVISORY COMMITTEE FOR AERONAUTICS

TECHNICAL NOTE 3498

EXPLORATORY INVESTIGATION OF AN AIRFOIL WITH AREA SUCTION APPLIED TO A POROUS, ROUND TRAILING EDGE FITTED WITH A LIFT-CONTROL VANE

By Robert E. Dannenberg and James A. Weiberg

SUMMARY

A two-dimensional, wind-tunnel investigation has been made of the effectiveness of area suction near the trailing edge for increasing the lift of an NACA 65_1-012 airfoil modified to incorporate a porous, round trailing edge. The modified section had a thickness-chord ratio of 0.16. A thin, small chord vane was located on the round trailing edge.

The results of the investigation indicate that with suction the vane was effective in controlling the lift without change in the angle of attack. The vane acted to fix the rear stagnation point and hence to control the circulation. Maximum lift for any given suction flow quantity was limited by leading-edge flow separation.

INTRODUCTION

Thwaites, in 1947, discussed the possibility of obtaining lift independently of the incidence of an airfoil (ref. 1). The method under consideration was to fix the location of the rear stagnation point by means of a thin vane which could be moved about a porous, round trailing edge through which suction was applied. Wind-tunnel experiments with a 3-inch-diameter, porous, circular cylinder fitted with a thin vane indicated that with suction, boundary-layer separation was prevented at small vane deflections and that the wake was completely suppressed. A maximum lift coefficient of about nine was attained for a vane deflection of 65°, and about four for a deflection of 30° (ref. 2).

In order to ascertain the effectiveness of this method of lift control applied to an airfoil, the present tests were made of a modified NACA 65_1-012 airfoil with a vane on a porous, round trailing edge.

Suction was applied and a vane was used to fix the rear stagnation point. The effects of variations of the chordwise extent of suction and of the vane geometry were investigated with the aim of attaining high maximum lift with low suction quantity.

NOTATION

c chord of model with vane, ft

c' chord of model without vane, ft

c_v vane chord, ft (See fig. 1(a).)

c_d section wake-drag coefficient, $\frac{\text{drag}}{q_o c}$, as determined from wake surveys, not including drag equivalent of suction power

c_l section lift coefficient, $\frac{\text{lift}}{q_o c}$

Δc_{l_s} value of c_l for a given model configuration with suction at a given angle of attack minus value of c_l for the same configuration without suction at the same angle of attack

c_m section pitching-moment coefficient, computed about 0.25c' for model with round trailing edge, $\frac{\text{pitching moment}}{q_o c^2}$

c_Q section flow coefficient, $\frac{w}{32.2\ \rho_o V_o c}$

H total pressure, lb/sq ft

$\frac{\Delta H}{q_o}$ total pressure-loss coefficient in wake, $\frac{H_o - H_{wake}}{q_o}$

Δh pressure difference across porous material, inches of water

P pressure coefficient, $\frac{p - p_o}{q_o}$

p static pressure, lb/sq ft

q_o free-stream dynamic pressure, $\frac{1}{2}\rho_o V_o^2$, lb/sq ft

R Reynolds number based on model chord

s	distance along airfoil surface, ft
V_o	free-stream velocity, fps
v	suction air velocity normal to outer surface of the airfoil, fps
w	weight rate of suction air flow per unit span, lb/sec
x	distance from airfoil leading edge measured parallel to chord line, ft
z	distance measured normal to chord line at 0° angle of attack, ft
α	section angle of attack, deg
$\frac{\Delta\alpha}{\Delta\delta}$	section aileron effectiveness parameter, ratio of change in section angle of attack to increment of aileron deflection at a constant value of lift coefficient
ρ	mass density of air, slugs/cu ft
δ	angular deflection of vane or flap, deg

Subscripts

e	local external point
o	free-stream conditions
1	conditions in suction duct
u	uncorrected
max	maximum
min	minimum

MODEL

The model used in this investigation was constructed to the profile of an NACA 65_1-012 airfoil with the rear portion modified for porous area suction as shown in figure 1(a). The resulting profile had a thickness-chord ratio of 0.16. The modified region extended from 93.5- to 100-percent chord. A fairing obtained by a conic lofting method was used in this region and, for convenience, this fairing will be called the round

trailing edge. Coordinates of the NACA 65_1-012 airfoil and of the airfoil with the round trailing edge are given in tables I and II. The model, mounted in one of the Ames 7- by 10-foot wind tunnels, spanned the 7-foot dimension of the test section as shown in figure 2.

The porous rear portion of the model consisted of a perforated metal sheet (0.016 inch thick) spot-welded to ribs spaced approximately 4.6 inches apart. The perforated sheet had 714, 0.020-inch-diameter holes per square inch which made its area 23 percent open. The sheet was backed with 1/8 inch of a commercial grade of felt. The felt was held against the surface sheet by a 12-mesh, 0.025-inch-diameter wire cloth supported by 1/8-inch-diameter rods which passed through the metal ribs as shown in figure 3. The chordwise extent and position of the porous region were varied by covering portions of the perforated sheet with a nonporous tape approximately 0.003 inch thick.

The rear portion of the model was constructed to accommodate the five vanes listed in figure 1(a). The vanes were usually placed normal to the surface at the positions and resultant deflection angles shown in figure 1(b). At each position, the vanes could also be set at various deflection angles in addition to the normal deflection shown. The vanes consisted of 1/16-inch-thick metal strips fastened by small hinged brackets to the porous area (see fig. 4). Each third rib in the trailing-edge portion was 1/4 inch thick to accommodate the vane brackets. The remaining ribs were 1/16 inch thick. The juncture between the vane and model surface was sealed with a nonporous tape.

For a deflection of 57°, two vanes were equipped with wood fairings to approximate the contours of plain flaps as shown in figure 1(c). The porous surface extended over a small region on the upper surface above the hinge line.

TESTS

Measurements of the lift and pitching moment were made with the wind-tunnel balance system. Tunnel-wall corrections computed by the method of reference 3 were applied to the data as follows:

$$\alpha = \alpha_u + 0.332c_{l_u} + 1.329c_{m_u}$$

$$c_l = 0.940c_{l_u}$$

$$c_m = 0.977c_{m_u} + 0.0092c_{l_u}$$

The wake pressures used in the calculation of the profile drag were measured by a rake of total- and static-pressure tubes one-quarter chord behind the model trailing edge. Unless otherwise noted, all tests were

made for a free-stream velocity of 162 feet per second (Mach number of 0.14) which for the 4.187-foot chord of the model with the round trailing edge corresponded to a Reynolds number of 4,200,000.

Air was drawn through the porous surface into a hollow spar in the wing (fig. 1(a)) and then through a ducting system by a suction pump outside the test chamber. A mercury seal isolated the model and the scale system from the mechanical forces that otherwise would have been imposed by the external ducting. The quantity of air flowing through the duct was measured by means of a standard A.S.M.E. orifice. The flow-resistance characteristics of the porous material were ascertained experimentally by the method described in reference 4 and are given in figure 5. The data presented for the suction-off condition ($c_Q = 0$) were obtained with the suction line sealed between the model and the suction pump.

RESULTS AND DISCUSSION

Model With Vane

Comparison with conventional airfoil.- Tests of the model with suction off ($c_Q = 0$) were made with several vane arrangements. The section characteristics for two typical arrangements are shown in figure 6. Comparison with data for the NACA 65_1-012 airfoil from reference 5, included in figure 6, indicates that the model with the 0.05c' vane had approximately the same lift and moment characteristics but a higher wake drag. Reducing the vane chord to 0.02c' or removing the vane adversely affected the lift and moment as well as the drag.

Data for the model with the 0.05c' vane at 0° with suction off indicate that within a range of Reynolds numbers from 2,100,000 to 4,800,000 the lift and moment characteristics were relatively unchanged.

In order to obtain an indication of the effect of rounding the trailing edge on the high-speed characteristics of the airfoil, the drag-divergence Mach number was computed from the pressure-distribution data using the crest-line method of reference 6. Rounding the trailing edge of the NACA 65_1-012 airfoil had no effect on the computed drag-divergence Mach number with suction off. Suction slightly decreased the critical Mach number at low values of lift coefficient.

Chordwise extent of porous area for maximum lift.- The test results presented herein were exploratory in nature with the primary object of gaining both an understanding of the mechanics of the flow and ascertaining the lift potentialities of the model arrangement. With suction off ($c_Q = 0$), the flow separated off the rear portion of the model resulting in the increased drag noted in figure 6. With suction applied, separation was prevented, and as will be discussed later in the report, the wake drag

was reduced below that of the basic airfoil. With a vane deflected and suction applied, large increases in lift were obtained with a corresponding build-up of peak negative pressure coefficients over the upper rear surface of the section. (For example note fig. 9(b).) The well-rounded trailing-edge section used on the model was selected to give a gradual transition from the basic airfoil contour to the trailing-edge radius so as to avoid excessive pressure "peaks" in this region. Large negative pressure coefficients increase the suction pressures against which a pump would have to operate with a resultant increase in the power required for suction.

Suction applied to the entire chordwise extent of the porous area (0.896 x/c' on upper surface to 0.935 x/c' on lower surface) was inefficient from the standpoint that large suction quantities were required for only small increases in the lift. Typical variations of the lift coefficient with section flow coefficient for the model with a 0.05c' vane deflected 57° are shown in figure 7. The effects of chordwise extent and location of the porous area on the lift at a fixed angle of attack were determined for a free-stream velocity of 163 feet per second. Because it was difficult to obtain consistent data at higher angles of attack, the flow characteristics are compared at 7° angle of attack.

Closing off the porous area on the lower surface upstream of the vane (porous opening from 0.896 x/c' on upper surface to 0.973 x/c' on lower surface) resulted in an increase in lift for a given value of c_Q (fig. 7). The increase in lift was due to increased flow through the upper surface. Closing off all the porous area on the lower surface (porous opening from 0.896 x/c' on upper surface to trailing edge) resulted in the largest increase in lift obtained for a given flow rate. Moving the upstream edge of the porous area downstream to the chordwise point of the minimum external pressure (0.941 x/c' on the upper surface) did not change the lift for a given c_Q but did result in a smaller extent of suction at a cost of increased suction air velocities.

The data of figure 7 were obtained while a constant angle of attack was maintained as the flow quantity was reduced from a high value to one close to zero. Tests made while the flow quantity was varied in the opposite direction showed no hysteresis. Data for the model with a 0.20c' vane deflected 57° showed similar trends.

Effects of suction.- Representative results are shown in figure 8 for the model with the minimum suction area for efficient lift control as noted from figure 7. The lift for a given angle of attack increased rapidly as the section flow coefficient was increased from zero. Increasing c_Q gradually reduced flow separation over the upper surface of the round trailing edge until the deleterious effects of separation on the lift were eliminated. Further increase in c_Q resulted in only very small increases in lift coefficient. For the purposes of this report, the lowest flow coefficient required to maintain unseparated flow on the round

trailing edge will be referred to as the separation-point c_Q. For the model with the 0.05c' vane, the separation-point c_Q was about 0.008 (fig. 8(a)). With additional increase in c_Q above this value, the lift increase appeared to be proportional to nc_Q with n between 20 and 25.

No attempt was made to reduce the separation-point c_Q by changing the chordwise distribution of the suction air velocities. The porous material (fig. 5) used in the model had a uniform permeability. Varying the chordwise distribution of permeability (for example, by the method of ref. 4) would alter the suction-velocity distribution. It is believed that substantial reductions in the separation-point c_Q could be realized with a tapered arrangement of chordwise permeability.

The shape of the lift curve at the stall and the pressure distributions in figure 9 indicate that maximum lift is limited by leading-edge flow separation. The peak negative pressure coefficients near the leading edge at $c_{l_{max}}$ increased but slightly with increased maximum lift (fig. 10). Further increases in maximum lift would be dependent on control of the leading-edge flow separation.

Lift and pitching-moment characteristics of the model for several vane arrangements are presented in figures 11, 12, 13, and 14[1] for section flow coefficients of 0 and 0.010. The value of 0.010 was selected as it is approximately the separation-point value. Typical effects of vane deflection, length and position on maximum lift, and the lift at zero angle of attack are summarized in figures 15, 16, and 17. It is evident that for the model with a vane, suction was effective in controlling the lift without change in the angle of attack. The vane acted to fix the rear stagnation pcint and hence to control the lift. It is noteworthy that for a given angle of attack the increase in section lift coefficient resulting from suction, Δc_{l_s}, for a suction quantity of 0.010, was relatively independent of the vane deflection or the vane chord. (See fig. 18.) The magnitude of this lift increment, as well as the maximum lift, decreased slightly as the vane position on the lower surface approached the trailing edge of the model (fig. 17). With a c_Q of approximately 0.010, the maximum lift coefficients of the model with the 0.05c' and 0.20c' vanes were 2.2 and 2.6, respectively. Higher values of maximum lift were attained with increased flow quantities as indicated in figure 8. The effects of the vane deflection, chord, and location on the pressure distributions for zero angle of attack are shown in figure 19. While pressures on the vane were not measured, it appears that the lift carried by the vane was quite small.

Wake drag.- The variation of section wake-drag coefficient with section lift coefficient is shown in figure 20(a) for the model with the 0.05c' vane ($\delta = 0^\circ$) and the porous area on the upper surface. The wake

[1]It should be noted that the lift coefficients in this report are based on a chord equal to that of the model with vane (see fig. 1(a)).

profiles shown in the figure are not located relative to the model chord line. With a c_Q of 0 the wake was steady. The values of c_d were greater than those for conventional 12- to 16-percent-thick airfoils. At an uncorrected angle of attack of -4°, increasing the section flow coefficient from 0 to approximately 0.003 resulted in a reduction in wake drag. Further increase in c_Q did not reduce the wake drag below 0.0063. As the suction air did not act directly on the boundary-layer flow over the lower surface, the wake drags were not reduced below values corresponding to the drag attributable to the lower surface without suction. Similar trends were noted for 0° angle of attack and to a lesser extent for 4° uncorrected angle of attack.

Another matter of interest which was investigated with this model was the question as to whether or not the wake could be entirely suppressed by suction. Tests indicated that with suction applied equally to both upper and lower surfaces around the trailing edge, the wake drag was reduced to exceedingly low values, as can be noted in figure 20(b). At zero angle of attack a wake-drag coefficient of 0.0002 was measured for a section flow coefficient of 0.0116. It is doubtful if the wake drag could be reduced to zero because of the wake arising from the 0.05c' vane.

Wake surveys behind the model with the 0.05c' vane deflected 57° indicated a nonuniform static pressure across the wake, particularly for a c_Q of 0. This variation was accounted for in computing c_d by the method discussed in reference 7. Two values of drag coefficient with corresponding values of minimum external and duct pressure coefficients for the model with the 0.05c' vane deflected 57° ($c_Q = 0.010$) are as follows:

α_u, deg	c_l	c_d	$P_{e_{min}}$ over porous surface	P_1
0	1.859	0.0186	-4.0	-5.6
4	2.108	.0297	-3.6	-5.2

Total drag.- The total section drag of the model is the sum of the wake drag and the suction drag. For a first approximation, the product $-c_Q P_1$ can be considered as the drag equivalent of the power required to pump the suction air back to free-stream static pressure. The magnitude of $-P_1$ is dependent on the external pressure coefficient on the porous surface and on the flow resistance of the permeable material. For the permeable material used in this investigation the total drag coefficients corresponding to the minimum wake-drag coefficients 0.0024 and 0.0002 (figs. 20(a) and (b)) would be 0.0312 and 0.0492, respectively. While low wake drag can be obtained by suction at the trailing edge, the necessary suction quantities as indicated by the present tests may be so large as to make the scheme uneconomical for drag reduction. However, lower required suction quantities may be possible by the use of permeability distributions other than the one used.

Model Without Vane

Because thin, near-elliptical airfoils are of possible interest for rotor blades for helicoptors,[2] autogyros, and convertiplanes for operation in the reverse-flow field at low advance ratios, tests were conducted on the model with the vane removed. The section characteristics of this airfoil without suction are compared with those with vanes and with the conventional airfoil in figure 6. With suction, the lift varied peculiarly, depending on the suction quantity and the location of the porous area (fig. 21). Even with a large suction quantity, the wake remained appreciable (fig. 22). The effects of the location of the porous region on the pressure distribution are shown in figure 23. The distribution for a c_Q of 0, as exemplified in figure 23(a), was not affected by the changes in location. It is apparent that a vane is essential with area suction on the round trailing edge to fix the rear stagnation point in order to obtain high lift efficiently.

Model With Faired Vane

The lift characteristics of the model with 0.05c' and 0.20c' vanes faired to approximate plain flaps are shown in figure 24. A comparison with figure 8 indicates that the addition of the fairings generally reduced slightly the lift for a given angle of attack. However, the lift increment due to suction Δc_{l_s} was unchanged as compared with the plain-vane values in figure 18. The data with faired vanes also indicate that Δc_{l_s} was relatively unchanged by the fairing, provided the c_Q was greater than the separation-point c_Q.

A brief investigation was made of the effect of roughness on the lift of the model with the 0.20c' faired vane deflected 57° ($c_Q = 0.010$). The addition of a strip of roughness (grade 60 carborundum powder) from the leading edge to 1.5-percent chord along the upper surface reduced the section lift coefficient 0.1 at negative angles of attack and decreased the maximum lift coefficient 0.4, as shown in figure 24(b). A similar roughness strip at 15-percent chord did not affect the section lift characteristics either with or without the leading-edge roughness.

---

[2]The authors wish to call attention to the following related report which is concerned with a theoretical study of an oval shaped airfoil with area suction and a thin vane for lift control: Arnold, L., and Yuan, S. W.: Investigation of the Thwaites Airfoil Principle as Applied to Helicopter Rotor Blades. WADC Tech. Rep. 53-497, Jan. 1954.

Control Surface

While the main purpose of this investigation was to determine the characteristics of the model with various vane arrangements as high-lift devices, the vanes could also be used as control surfaces. In order to afford a comparison of various model arrangements as controls, values of $\Delta\alpha/\Delta\delta$ are presented in figure 25. Also shown in the figure are the theoretical values (from ref. 5) based on the extended length of the vane as measured from the model chord line. With the 0.05c' vane deflected 20° ($c_Q = 0.010$), the control-surface effectiveness was about the same as for a 17-percent-chord aileron without suction.

Comparison With Similar Lift-Control Devices

Ellipse with a vane.- The lift of elliptic cylinders in potential flow can be calculated and is used as a basis for judging the effectiveness of the vane in fixing the rear stagnation point and, hence, in controlling the lift. Typical lift results for the model with a vane at zero angle of attack are compared with calculated values for elliptic cylinders in figure 26. The rear portion of the model with the round trailing edge (without vane) approximated part of an elliptic cylinder having a thickness ratio of about 0.17. The data in figure 26 indicate that with the 0.05c' vane normal to the surface and a high suction flow rate, a close approximation to potential theory value was attained. Data are presented in reference 8 for a 35-percent-thick elliptical profile and in reference 2 for a circular cylinder with suction over the rear portions of both models. Vanes of various lengths were located on the lower surfaces, resulting in arrangements similar to that of the model with a vane used in this investigation. A comparison of the lift attained at zero angle of attack with the different profile shapes, as shown in figure 27, indicates that with the leading edges of the vanes at 0.94 x/c' the lift decreased with decreasing profile thickness ratio. A similar trend was noted in Δc_{l_s}. For the 35-percent-thick ellipse, Δc_{l_s} at the separation-point c_Q was about 1.6 as compared to 1.2 for the 16-percent-thick section used in this investigation. The maximum lift coefficients of the three profiles shown in figure 27 (based on the chord of the profile plus the chord of the vane) were as follows:

Profile	$c_{l_{max}}$	α for $c_{l_{max}}$
Circular cylinder		
$\delta = 28^\circ 11'$	3.8	---
$\delta = 60^\circ$	6.7 (max)	---
35-percent-thick ellipse	5.8	40°
NACA 651-012 with round trailing edge	2.57	3°

The maximum lifts given in the preceding table for the 65_1-012 airfoil with a round trailing edge were limited by flow separation from the leading edge. For the other profiles, the lifts given are the maximum obtained with the suction quantities available.

Trailing-edge suction slots.- Results similar to those for the model with the vane were noted from data for airfoils of comparable thickness utilizing suction slots at the trailing edge (refs. 9 to 12). For the arrangements shown in figure 28, the lift increases due to suction, for suction quantities above the separation-point values, were of the same magnitude. While the slot on the model with slot suction represents the optimum shape for lift control, improvement in the chordwise distribution of permeability for the model with area suction would reduce the separation-point c_Q. Although both systems yield similar lift gain for large suction quantities, area suction has the advantage of affording appreciable lift control for small flow rates.

The similarity in lift between the arrangements shown in figure 28 can be explained by considering the flow into the slot at the trailing edge. As suction is first applied, the boundary layer on the upper surface is gradually taken into the slot. Without suction, the boundary layer separates from the outer surface upstream of the slot. With increasing suction the separation point on the surface approaches the trailing edge and passes into the slot. A limiting streamline then exists between the suction flow and the free air, giving the airfoil, in effect, a round trailing edge with the circulation fixed by the split flap acting as a forced stagnation point. The lift increase for larger flow rates, as for the model with the round trailing edge, was about proportional to $22c_Q$.

The lift increment resulting from suction was only slightly affected by the split-flap deflection angle as noted from figure 28(b). With the vane and flap removed, section lift coefficients of 1.0 (slot suction) and 1.1 (area suction) were obtained for the respective models at zero angle of attack and a c_Q of 0.010. The suction pressures required to induce a c_Q of 0.010 for either model were approximately the same.

CONCLUDING REMARKS

Results have been presented of an exploratory wind-tunnel investigation of the effectiveness of area suction in combination with a vane on an NACA 65_1-012 airfoil with a round, porous trailing edge.

Section lift coefficients of 1.9 were obtained for a 5-percent-chord vane and 2.5 for a 20-percent-chord vane deflected 57° at zero angle of attack (c_Q = 0.010). With suction off, the respective lift coefficients were 0.7 and 1.5. For efficient lift control, the porous region should extend from the point of minimum external pressure over the rear portion of the model to the trailing edge.

Without suction the flow separated from the round trailing edge. Increasing suction gradually reduced flow separation over the round trailing edge until the deleterious effects of separation were eliminated. Further increase in c_Q resulted in only very small increases in lift coefficient. The major portion of the lift induced by the vane was carried on the airfoil.

The maximum lift for any given flow quantity was limited by leading-edge stall. This would make further increases in maximum lift dependent on control of the leading-edge separation.

Ames Aeronautical Laboratory
National Advisory Committee for Aeronautics
Moffett Field, Calif., Feb. 9, 1955

REFERENCES

1. Thwaites, B.: The Production of Lift Independently of Incidence - The Thwaites Flap, Parts I and II. R.& M. No. 2611, British A.R.C., 1947.

2. Pankhurst, R. C., and Thwaites, B.: Experiments on the Flow Past a Porous Circular Cylinder Fitted With a Thwaites Flap. R. & M. No. 2787, British A.R.C., 1953.

3. Allen, H. Julian, and Vincenti, Walter G.: Wall Interference in a Two-Dimensional-Flow Wind Tunnel, With Consideration of the Effect of Compressibility. NACA Rep. 782, 1944.

4. Dannenberg, Robert E., Weiberg, James A., and Gambucci, Bruno J.: A Fibrous-Glass Compact as a Permeable Material for Boundary-Layer-Control Applications Using Area Suction. NACA TN 3388, 1955.

5. Abbott, Ira H., von Doenhoff, Albert E., and Stivers, Louis S., Jr.: Summary of Airfoil Data. NACA Rep. 824, 1945.

6. Nitzberg, Gerald E., and Crandall, Stewart: A Study of Flow Changes Associated With Airfoil Section Drag Rise at Supercritical Speeds. NACA TN 1813, 1949.

7. Baals, Donald D., and Mourhess, Mary J.: Numerical Evaluation of the Wake-Survey Equations for Subsonic Flow Including the Effect of Energy Addition. NACA WR L-5, 1945.

8. Golden, J., House, W. C., and Johansen, H. V.: Low-Speed-Flight Research Program, Analysis Report, Series II - Wind Tunnel Tests. Rep. 509, Aerojet Eng. Corp., Azusa, Calif., Jan. 13, 1951.

9. Regenscheit, B.: Tests on a Wing With Suction at the Trailing Edge. British Rep. and Trans. No. 477, Jan. 1947, Völkenröde, Ref: FB 1594.

10. Hazen, D. C., Sweeney, T. E., Lehnert, R. F., and Ringleb, Friedrich O.: Circulation Control by Means of Trailing Edge Suction. Princeton Univ., Dept. Aero. Eng., Rep. 239, Aug. 31, 1953.

11. Heugham, D. M.: An Experimental Study of a Symmetrical Aerofoil With a Rear Suction Slot and a Retractable Flap. Jour. Royal Aero. Soc., Oct. 1953, pp. 627-645.

12. Ehlers, F.: On the Influence of Sinks on the Lift and Pressure Distribution of Airfoils With Suction Slots. British Rep. and Trans. No. 189, M.A.P. Völkenröde VG 67, Sept. 1946.

TABLE I.- COORDINATES FOR THE NACA 65_1-012 AIRFOIL SECTION
[Percent airfoil chord]

Station	Ordinate
0	0
.5	.923
.75	1.109
1.25	1.387
2.5	1.875
5.0	2.606
7.5	3.172
10	3.647
15	4.402
20	4.975
25	5.406
30	5.716
35	5.912
40	5.997
45	5.949
50	5.757
55	5.412
60	4.943
65	4.381
70	3.743
75	3.059
80	2.345
85	1.630
90	.947
95	.356
100	0
L.E. radius: 1.000	

TABLE II.- COORDINATES FOR THE MODIFIED NACA 65_1-012 AIRFOIL SECTION WITH A ROUND TRAILING EDGE
[Percent of conventional airfoil chord of table I]

Station	Ordinate
0	0
.5	.923
.75	1.109
1.25	1.387
2.5	1.875
5.0	2.606
7.5	3.172
10	3.647
15	4.402
20	4.975
25	5.406
30	5.716
35	5.912
40	5.997
45	5.949
50	5.757
55	5.412
60	4.943
65	4.381
70.00	3.743
70.70	3.612
71.18	3.492
71.73	3.248
72.24	3.075
72.71	2.821
73.13	2.552
73.58	2.254
74.17	1.687
74.33	1.493
74.58	1.179
74.77	.821
75.00	0
L.E. radius: 1.000	

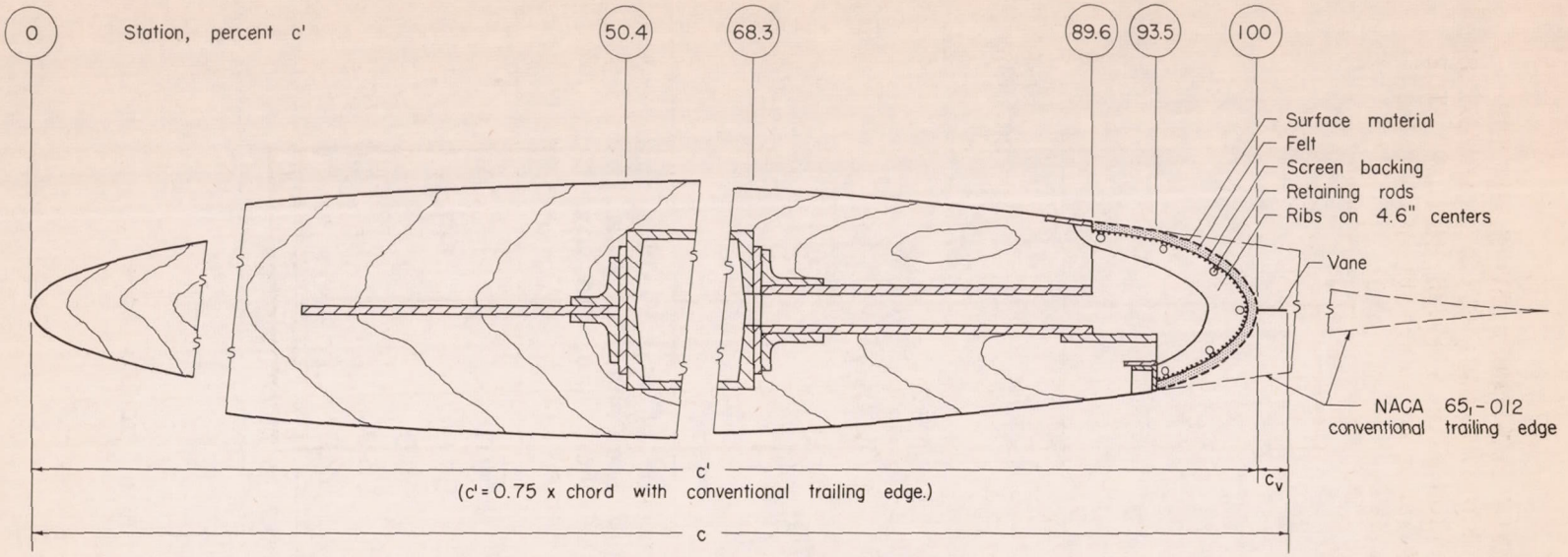

c, feet	Vane chord, c_v	
	Percent of c	Percent of c'
4.208	0.49	0.5
4.271	1.95	2
4.396	4.74	5
4.604	9.10	10
5.025	16.67	20
c' = 4.187 ft		

(a) Round trailing-edge control-vane combination.

Figure 1.- Geometry and reference dimensions for model.

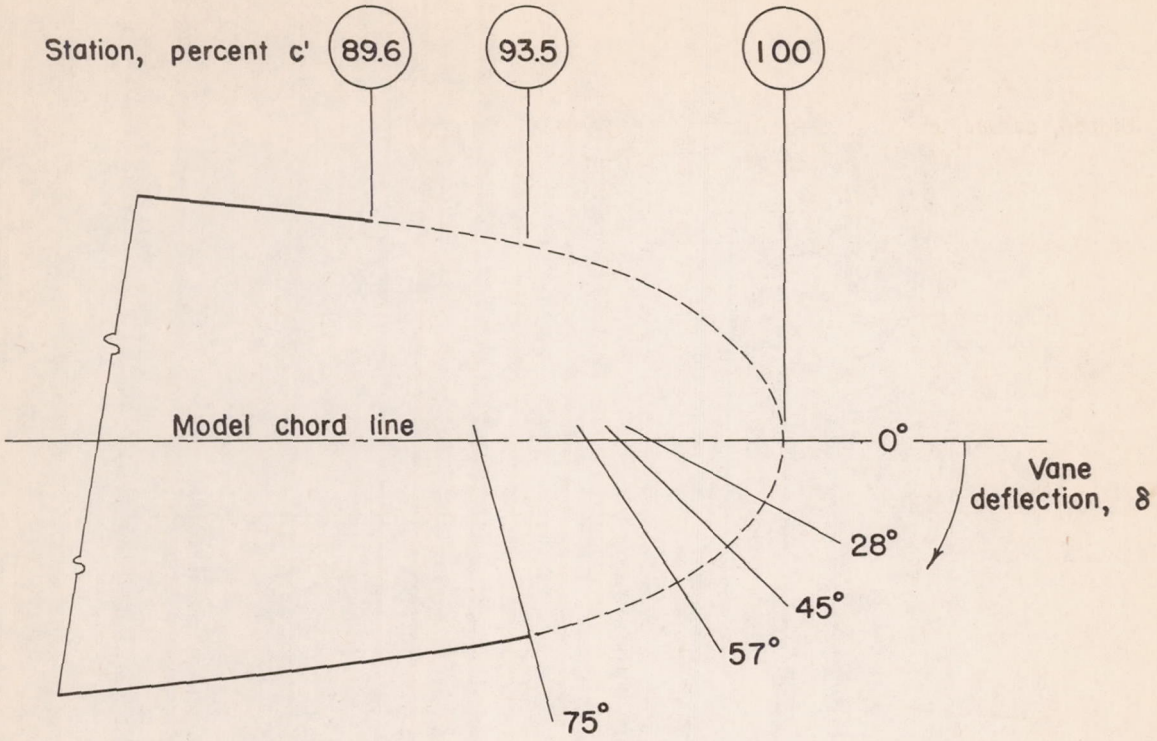

Vane deflection δ, deg	Intersection of vane chord line* with model surface, percent c'	Intersection of vane chord line with model chord line, percent c'	Surface distance from model chord line to vane chord line, percent c'
0	100.0	100.0	0
28	99.5	96.5	1.6
45	98.5	96.0	3.1
57	97.3	95.0	4.6
75	93.5	92.2	8.6

*Vane chord lines are normal to model surface

(b) Vane positions on round trailing edge.

Figure 1.- Continued.

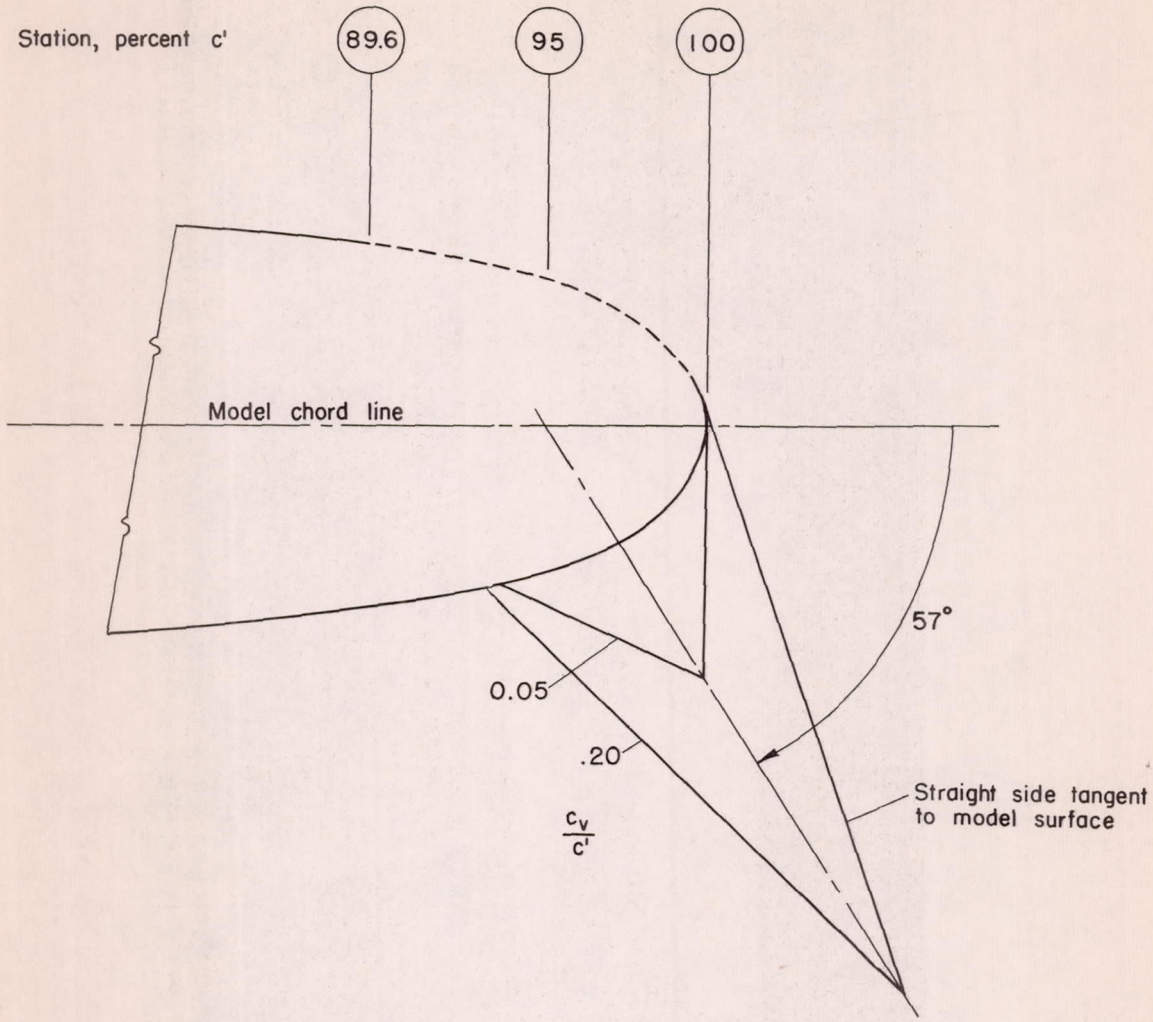

(c) Faired vane arrangement.

Figure 1.- Concluded.

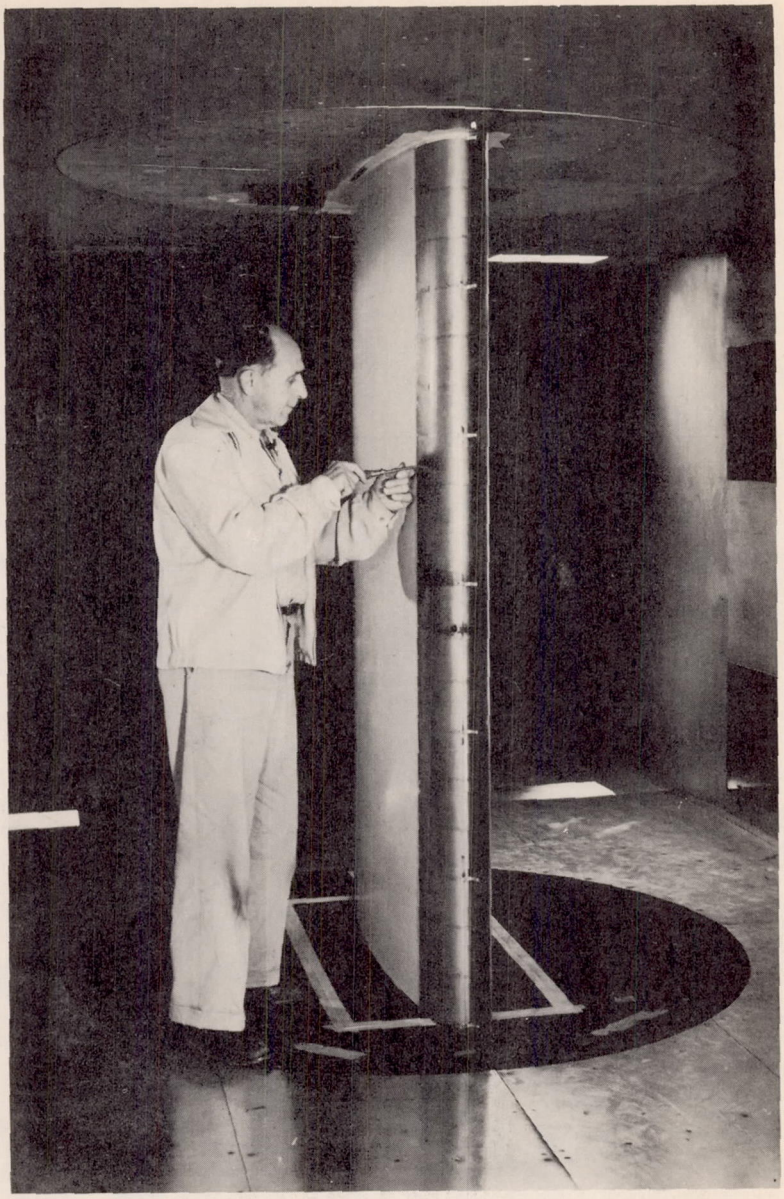

A-18689

Figure 2.- The NACA 65_1-012 airfoil with a porous, round trailing edge and a 5-percent-chord vane deflected 28°.

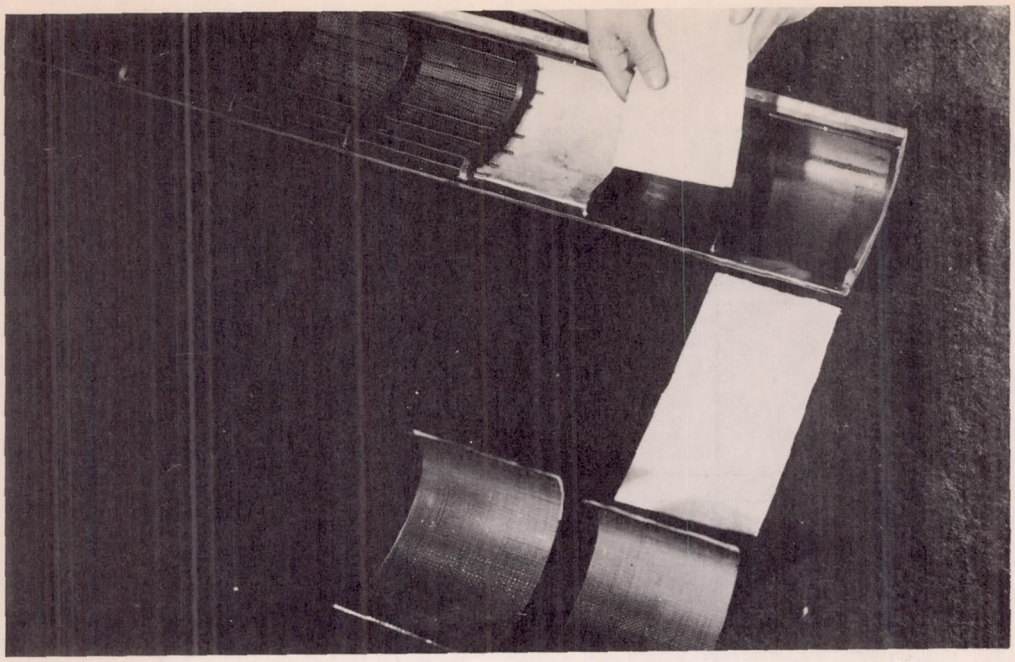

A-18926

Figure 3.- Typical arrangement of the permeable material (felt) in the perforated-sheet trailing-edge section.

A-18927

Figure 4.- Detail of vane and bracket construction.

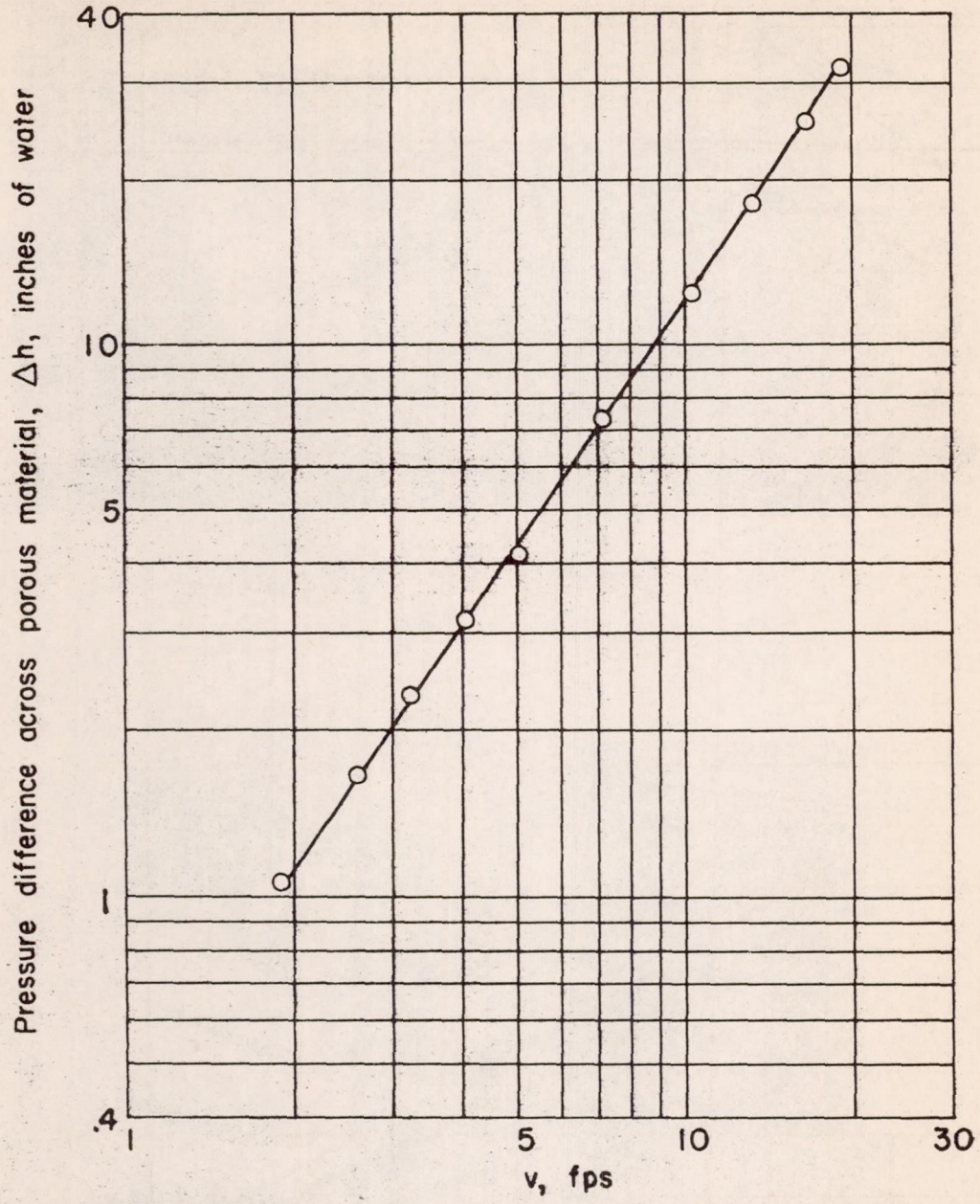

Figure 5.- Resistance to air flow of the perforated plate backed by felt cloth.

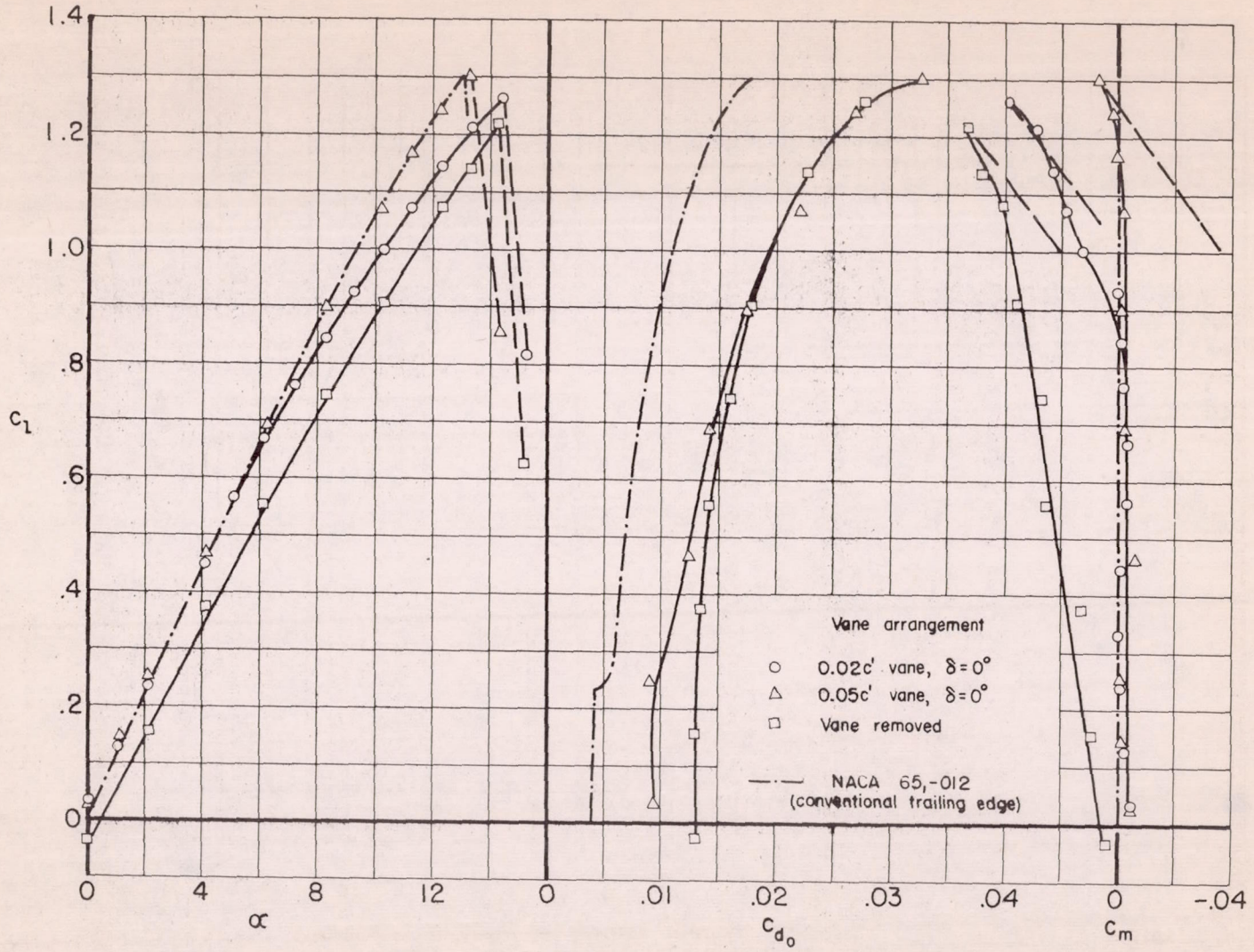

Figure 6.- Section aerodynamic characteristics of the model without suction; R = 4.3×10^6.

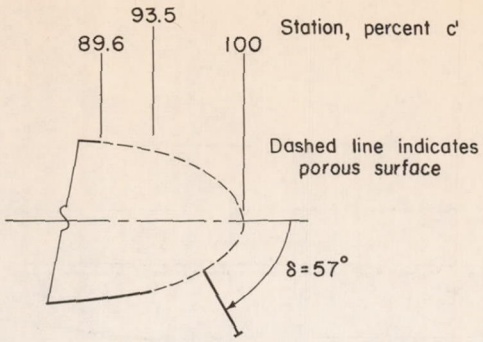

	Porous opening, x/c'			Distance along surface, s/c'
	Upper surface	to	Lower surface	
○	0.896		0.935	0.211
△	.896		.973	.171
	Upper surface only			
□	.896		1.0	.129
▽	.916		1.0	.110
◇	.941		1.0	.083
⌂	.980		1.0	.042
◿	.896		.985	.109
⌂	.941		.985	.068

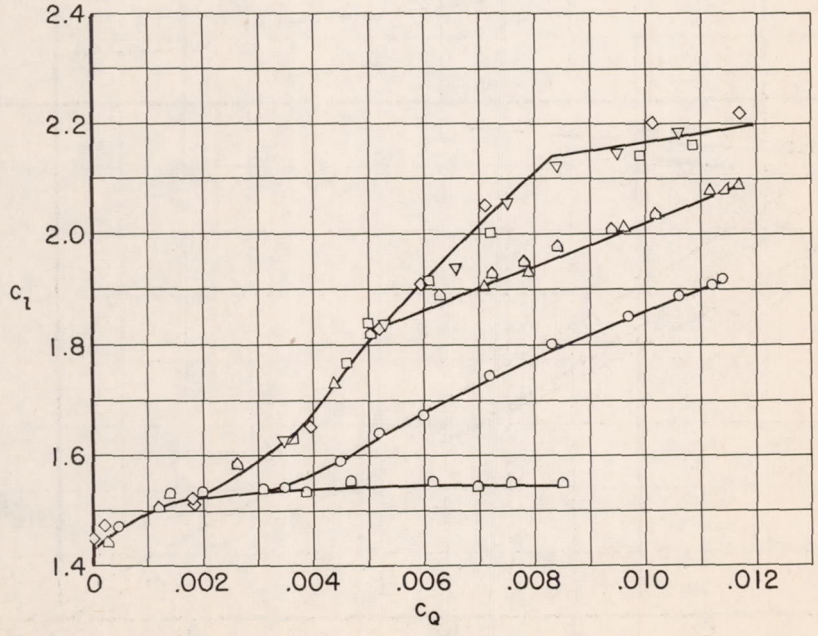

Figure 7.- Effect of location and extent of suction on section lift coefficient; model with 0.05c' vane; $\delta = 57^\circ$; $\alpha_u = 7^\circ$; $V_o = 163$ fps.

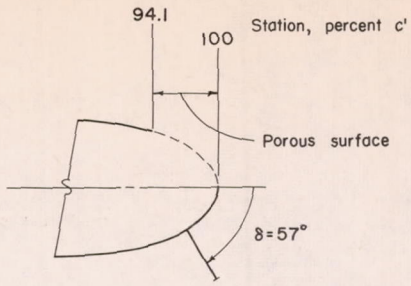

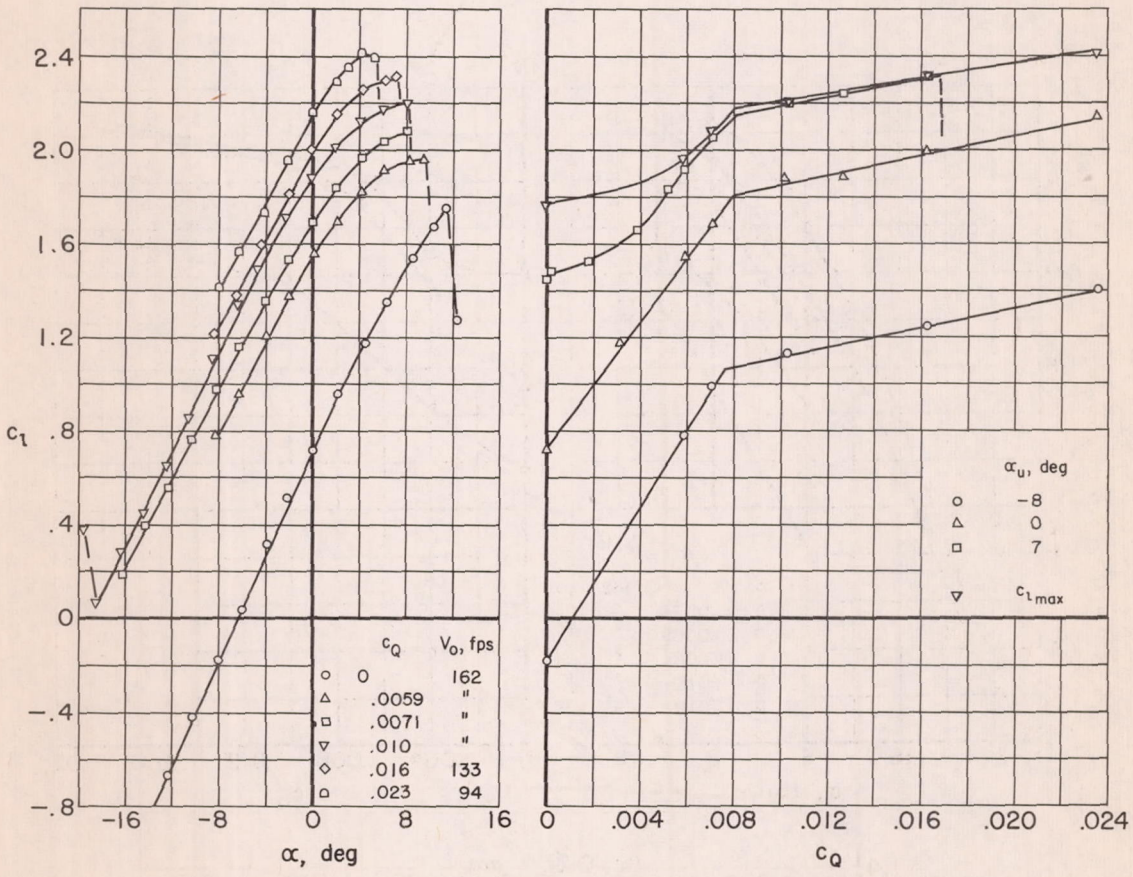

(a) 0.05c' vane

Figure 8.- Lift and flow characteristics for the model; porous area from 0.941c' on upper surface to trailing edge; $\delta = 57^{\circ}$.

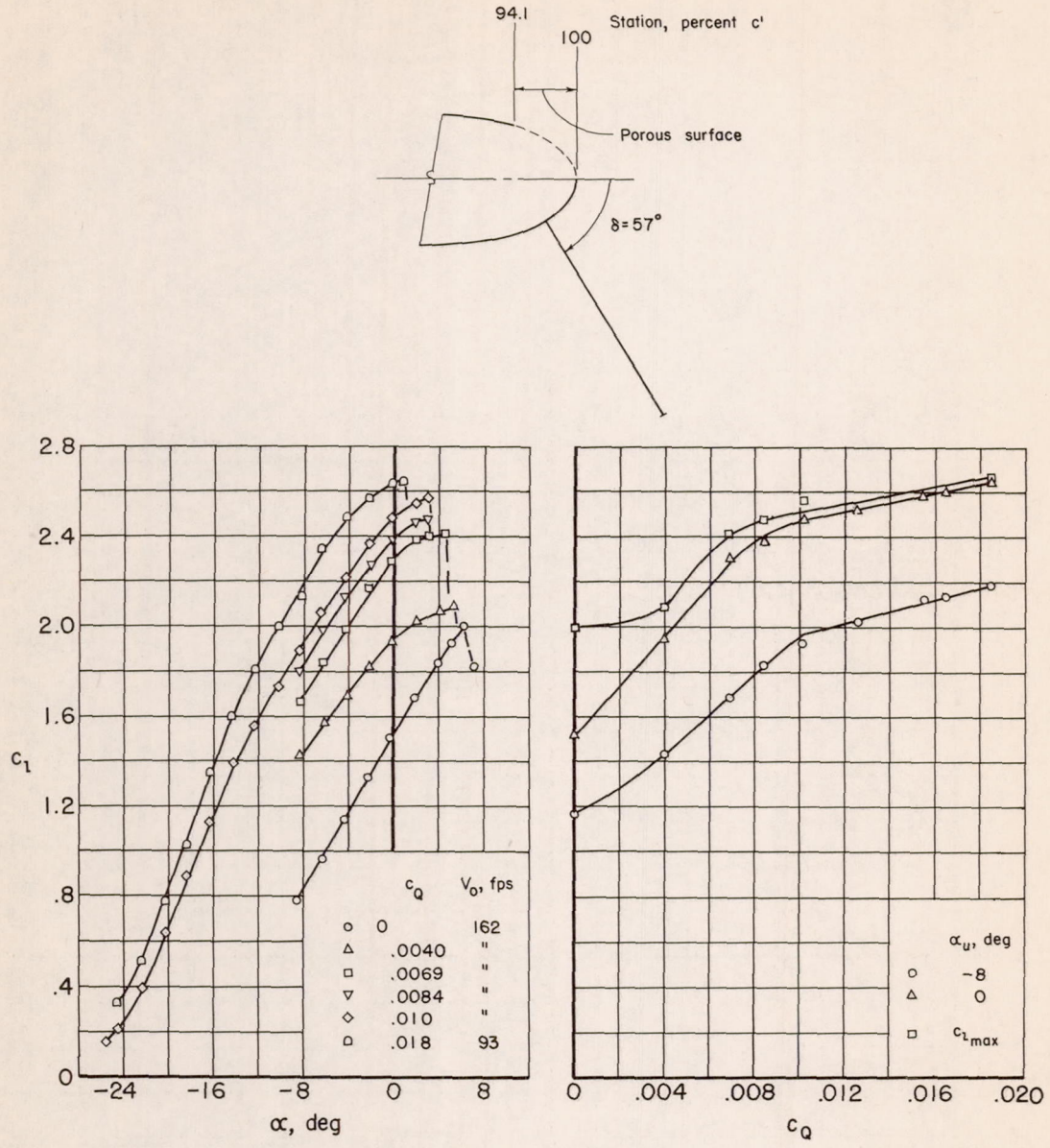

(b) 0.2c' vane

Figure 8.- Concluded.

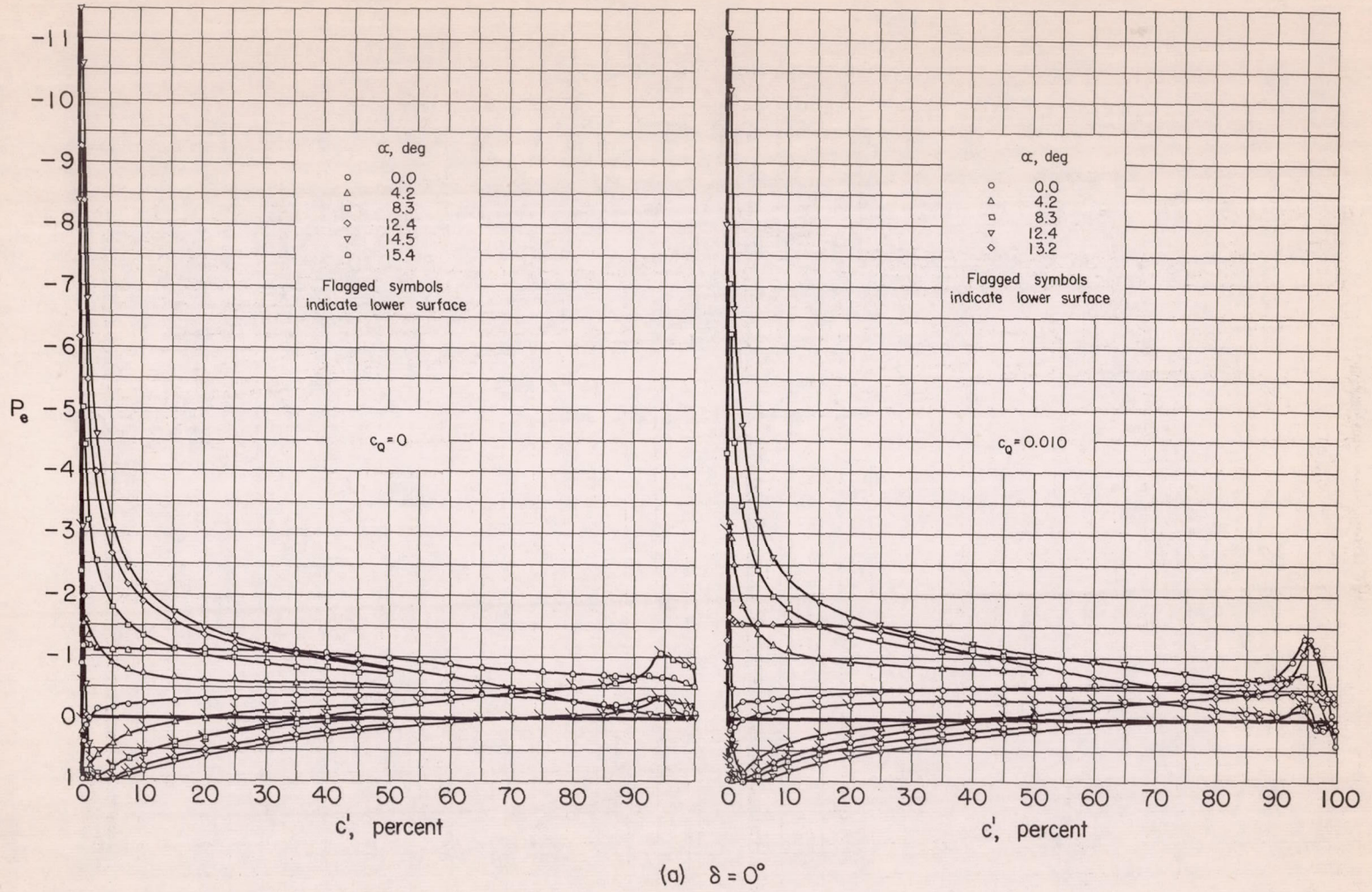

(a) $\delta = 0°$

Figure 9.- Chordwise distribution of pressure for the model with the 0.05c' vane normal to the surface; porous area from 0.941c' on upper surface to trailing edge.

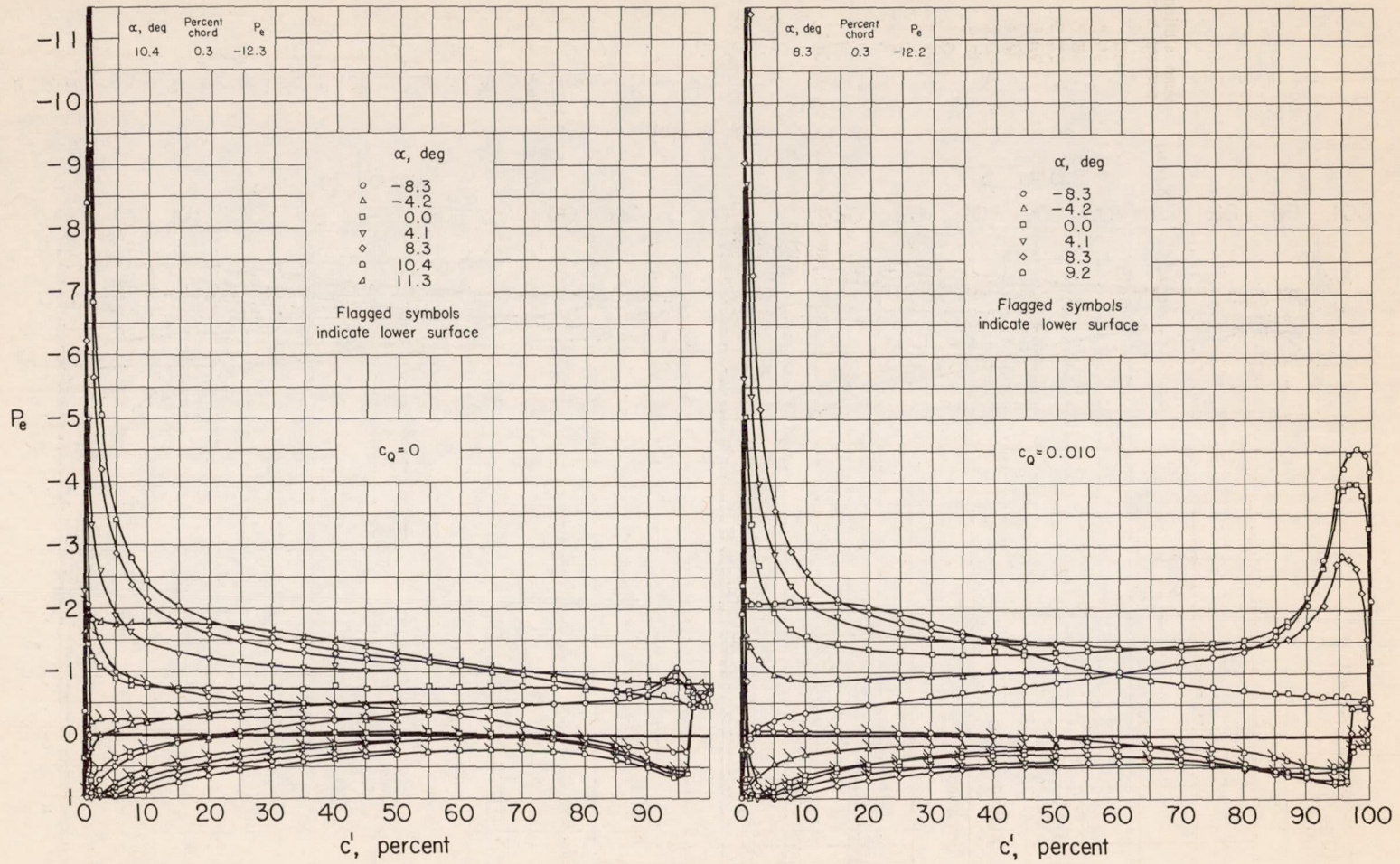

(b) $\delta = 57°$

Figure 9.- Concluded.

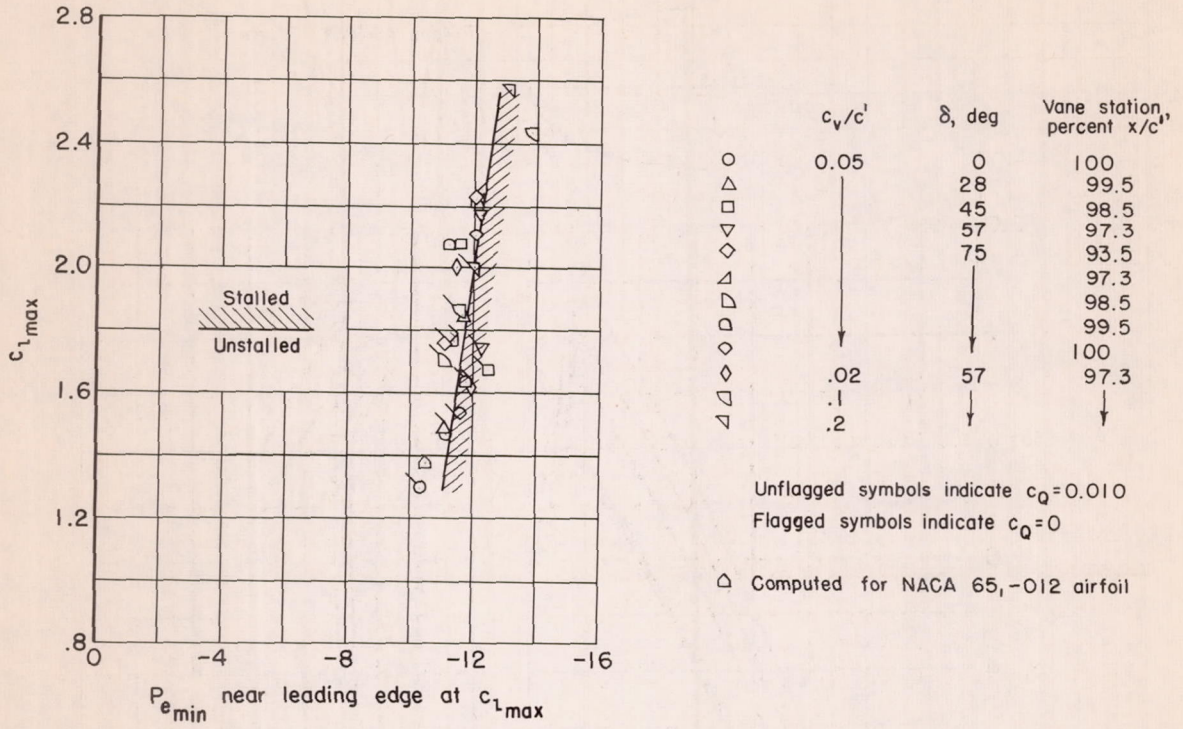

Figure 10.- Variation of minimum pressure coefficient with maximum lift coefficient; porous area from 0.941c' on upper surface to trailing edge.

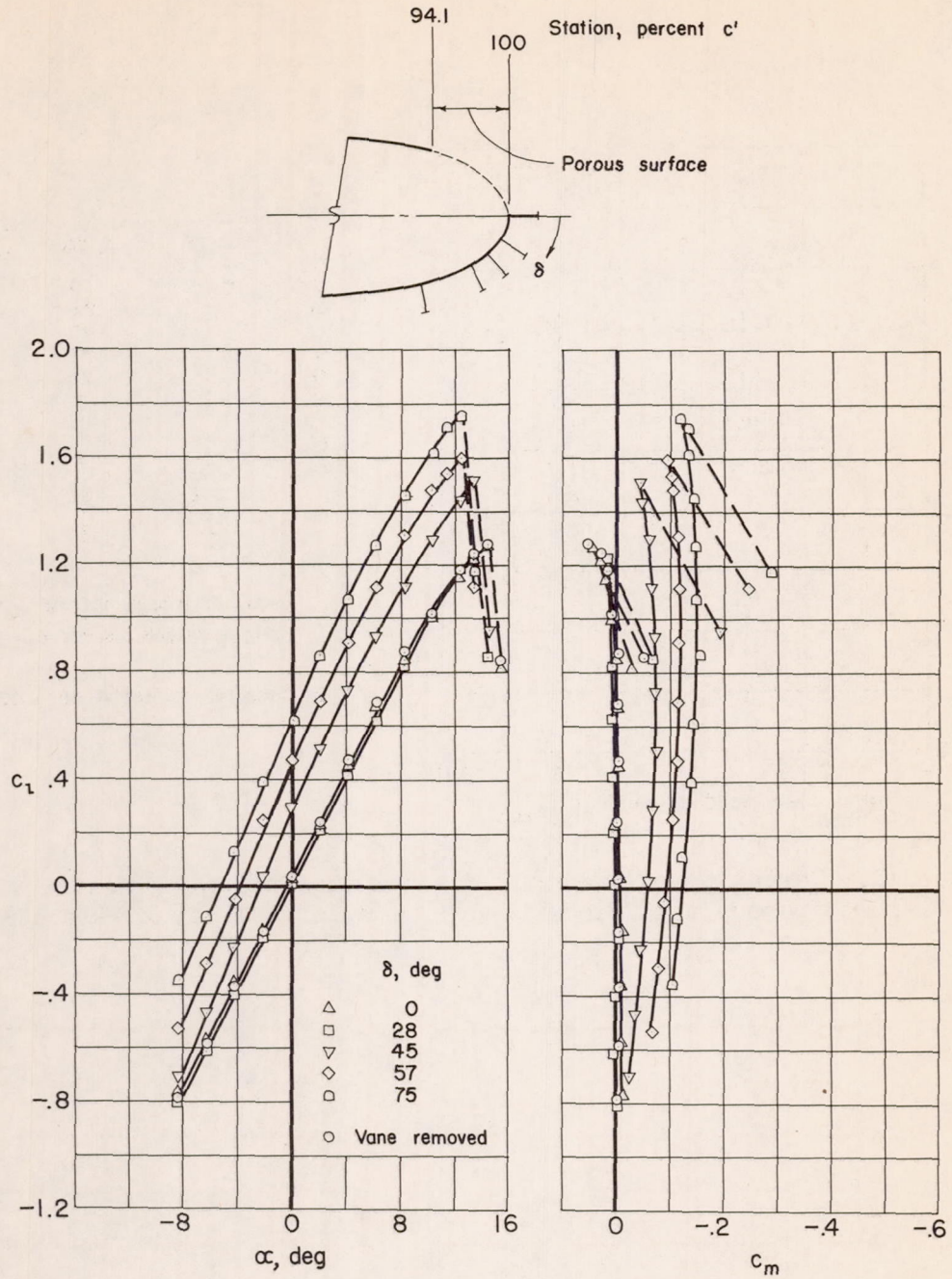

(a) $c_Q = 0$

Figure 11.- Section lift and pitching-moment coefficients for the model with the 0.02c' vane; porous area from 0.941c' on upper surface to trailing edge.

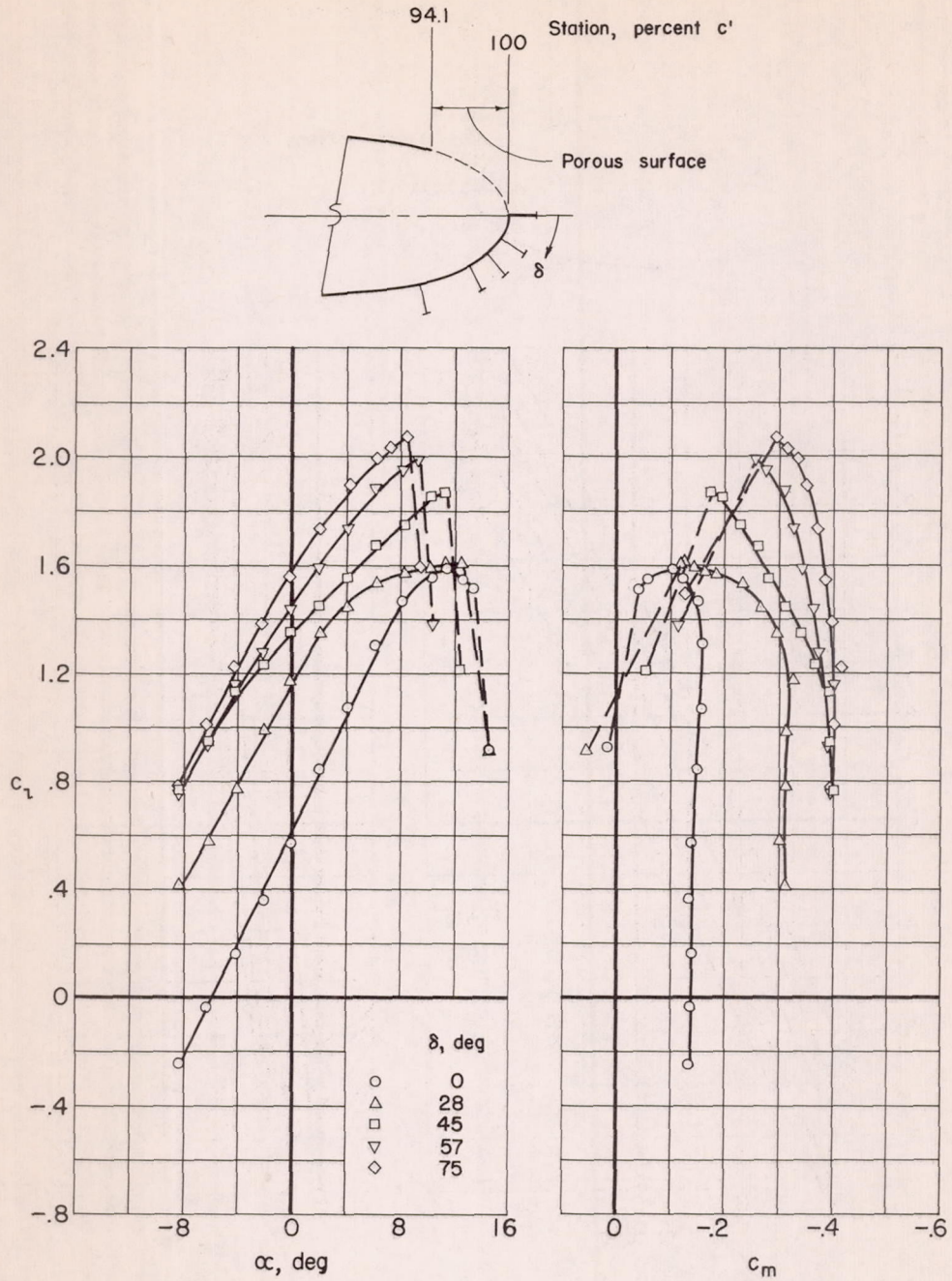

(b) $c_Q = 0.010$

Figure 11.- Concluded.

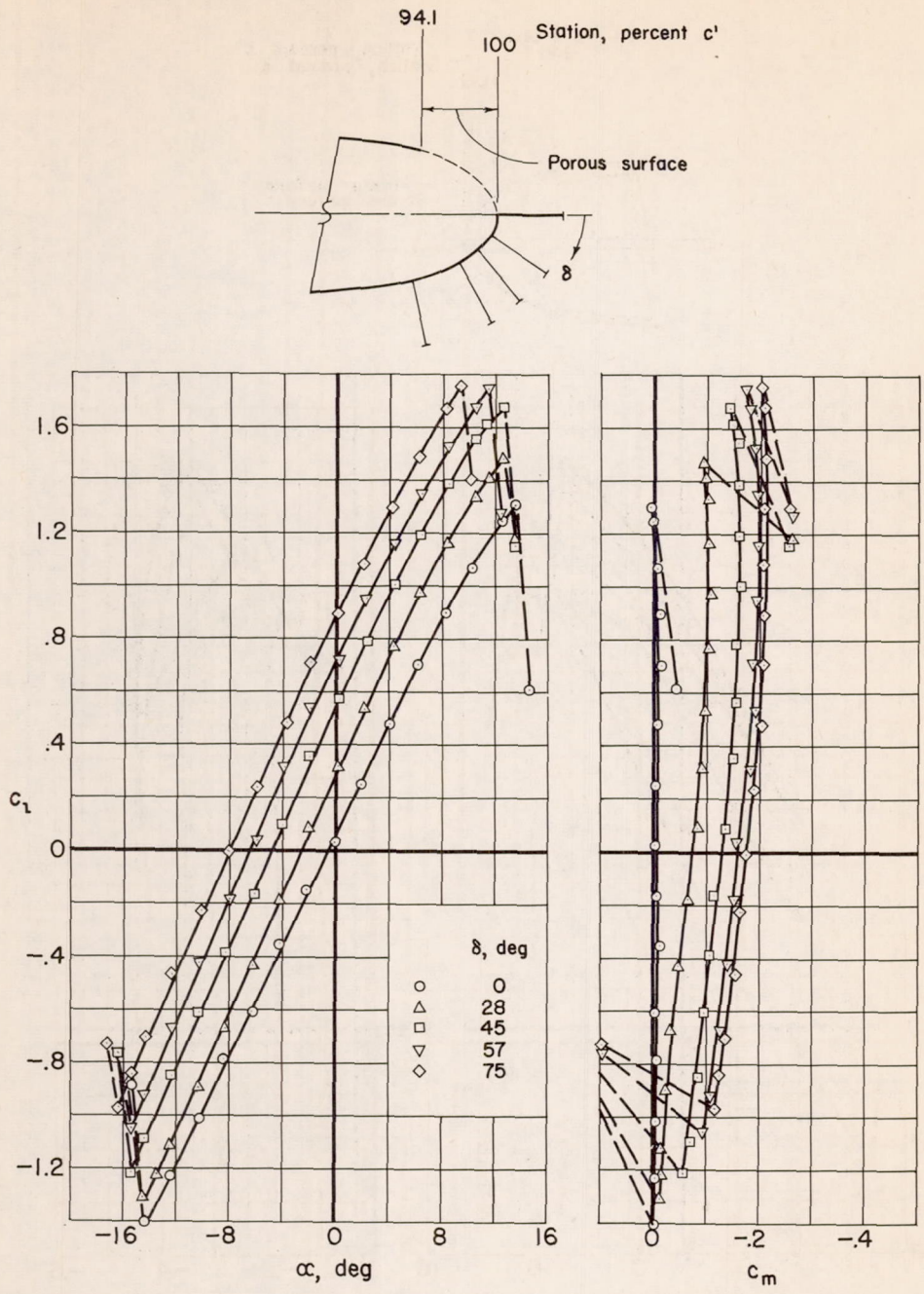

(a) $c_Q = 0$

Figure 12.- Section lift and pitching-moment coefficients for the model with the 0.05c' vane; porous area from 0.941c' on upper surface to trailing edge.

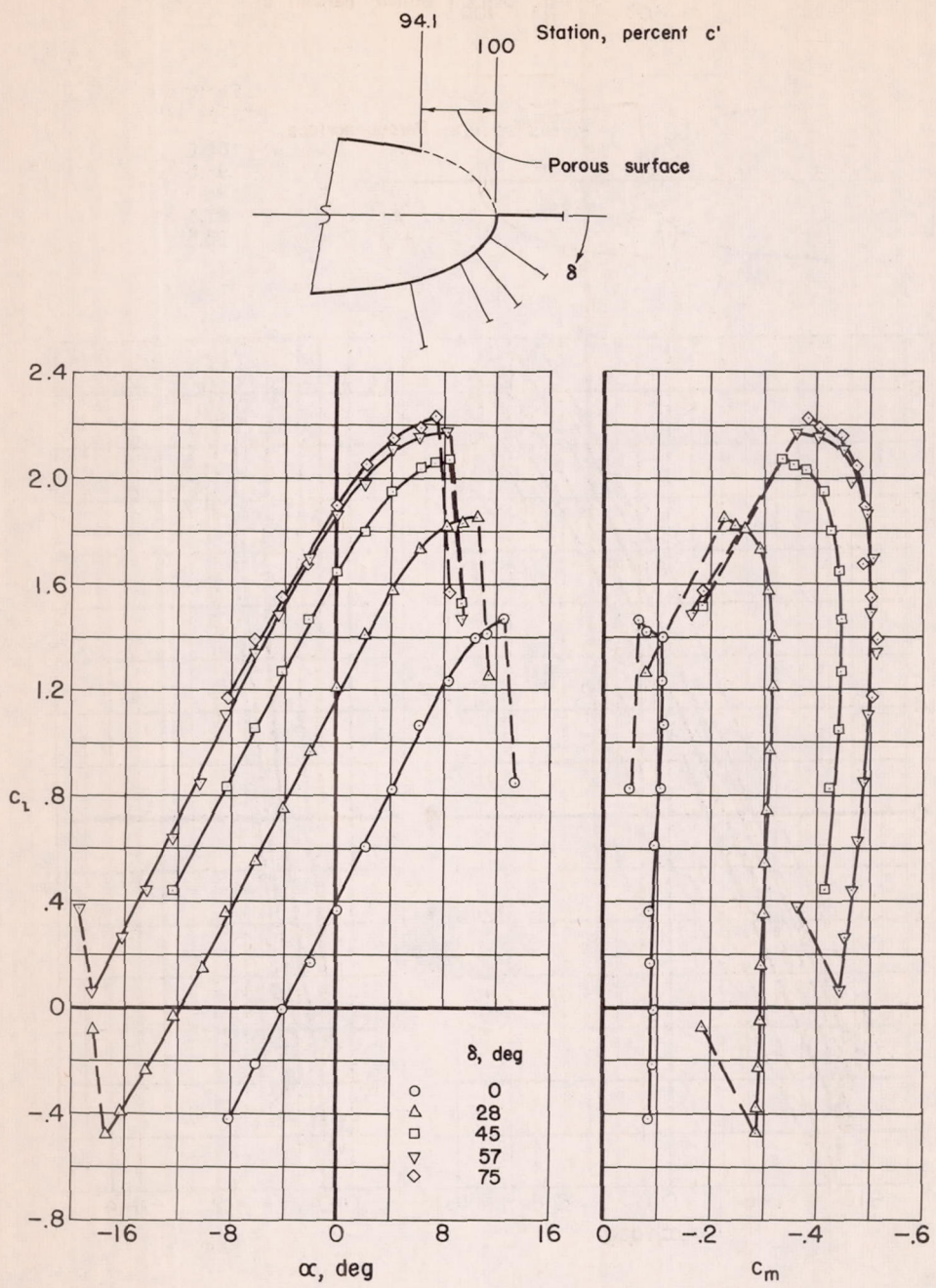

(b) $c_Q = 0.010$

Figure 12.- Concluded.

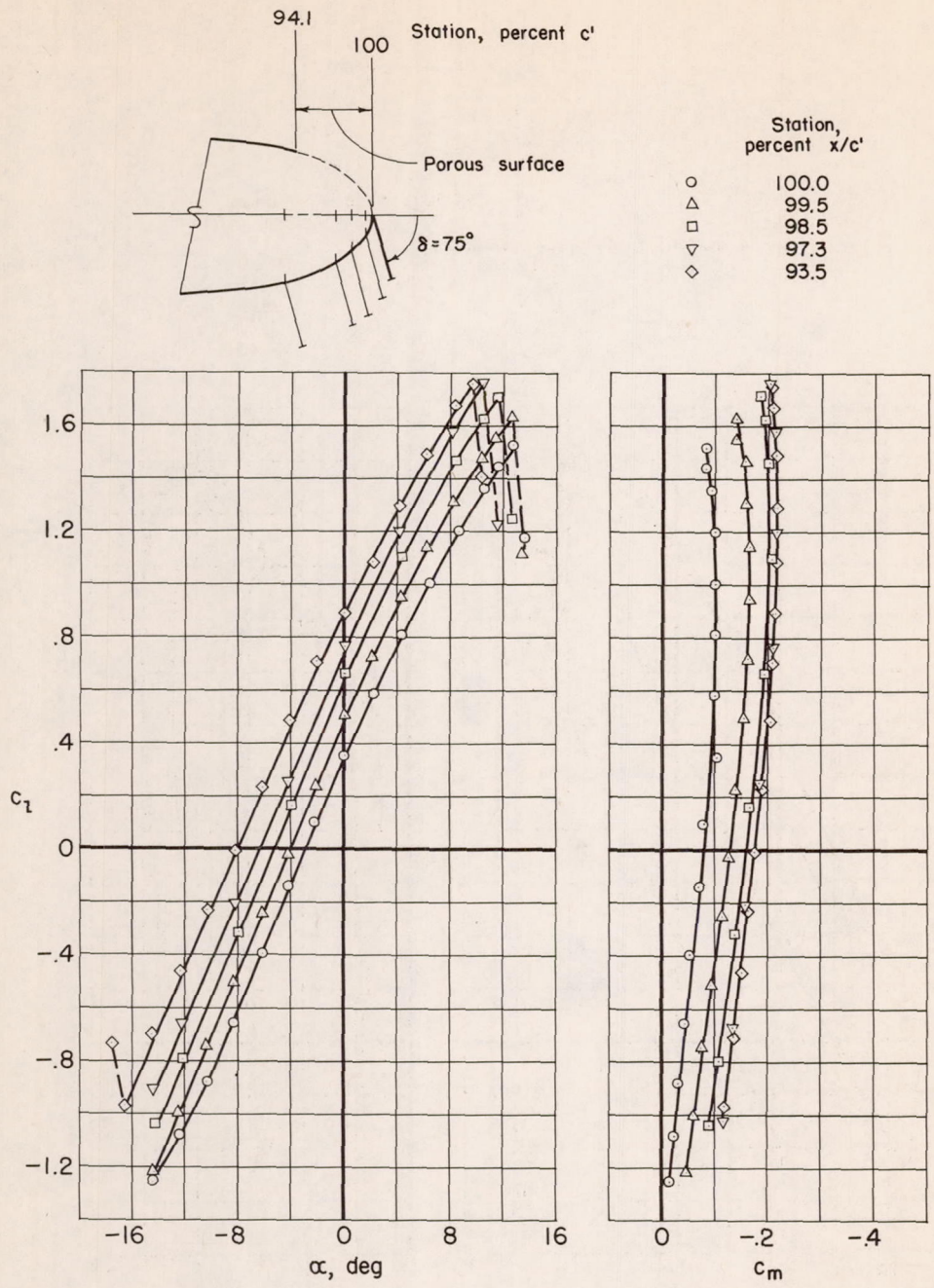

(a) $c_Q = 0$

Figure 13.- Section lift and pitching-moment coefficients for the model with the 0.05c' vane at various chordwise stations; $\delta = 75^\circ$; porous area from 0.941c' on upper surface to trailing edge.

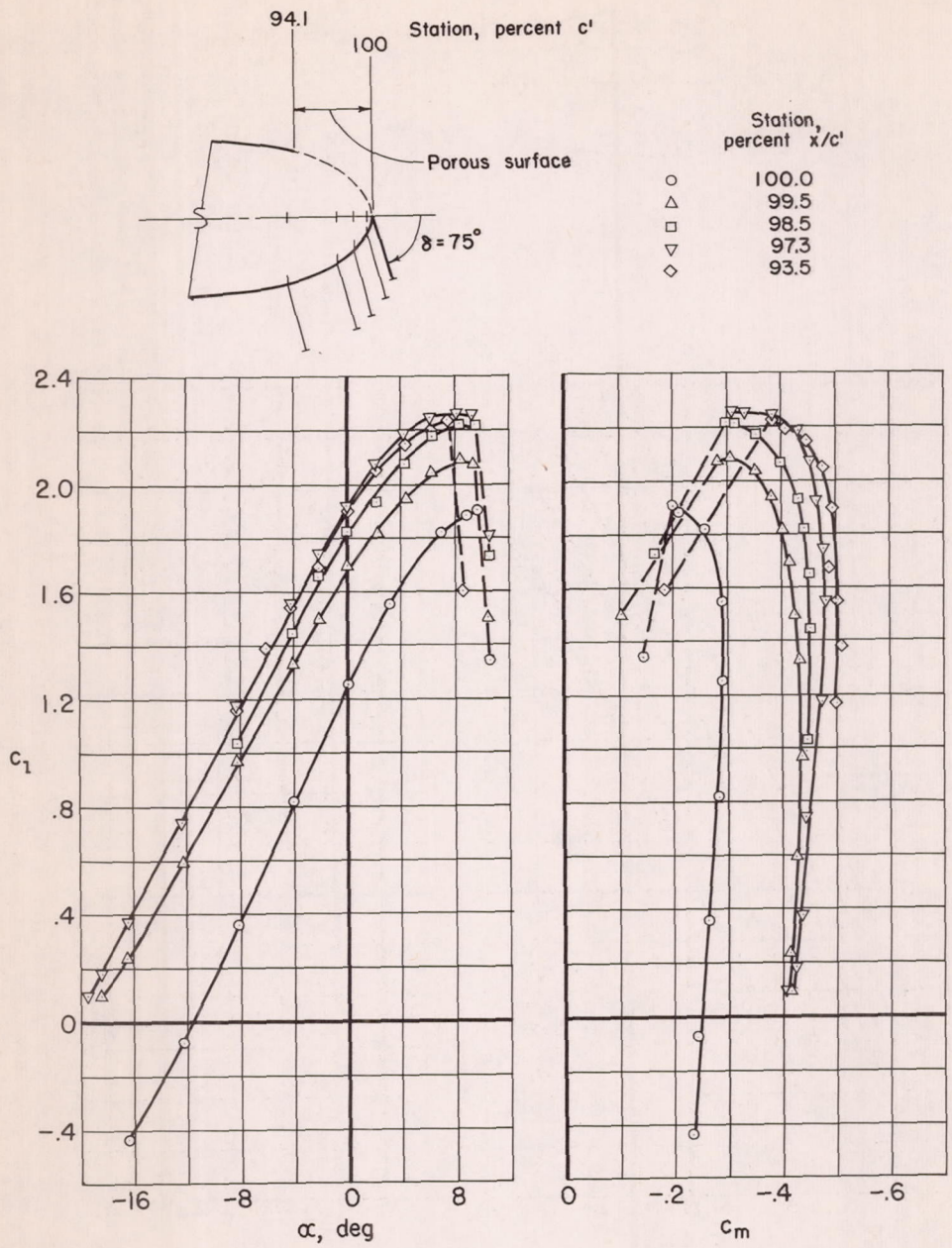

(b) $c_Q = 0.010$

Figure 13.- Concluded.

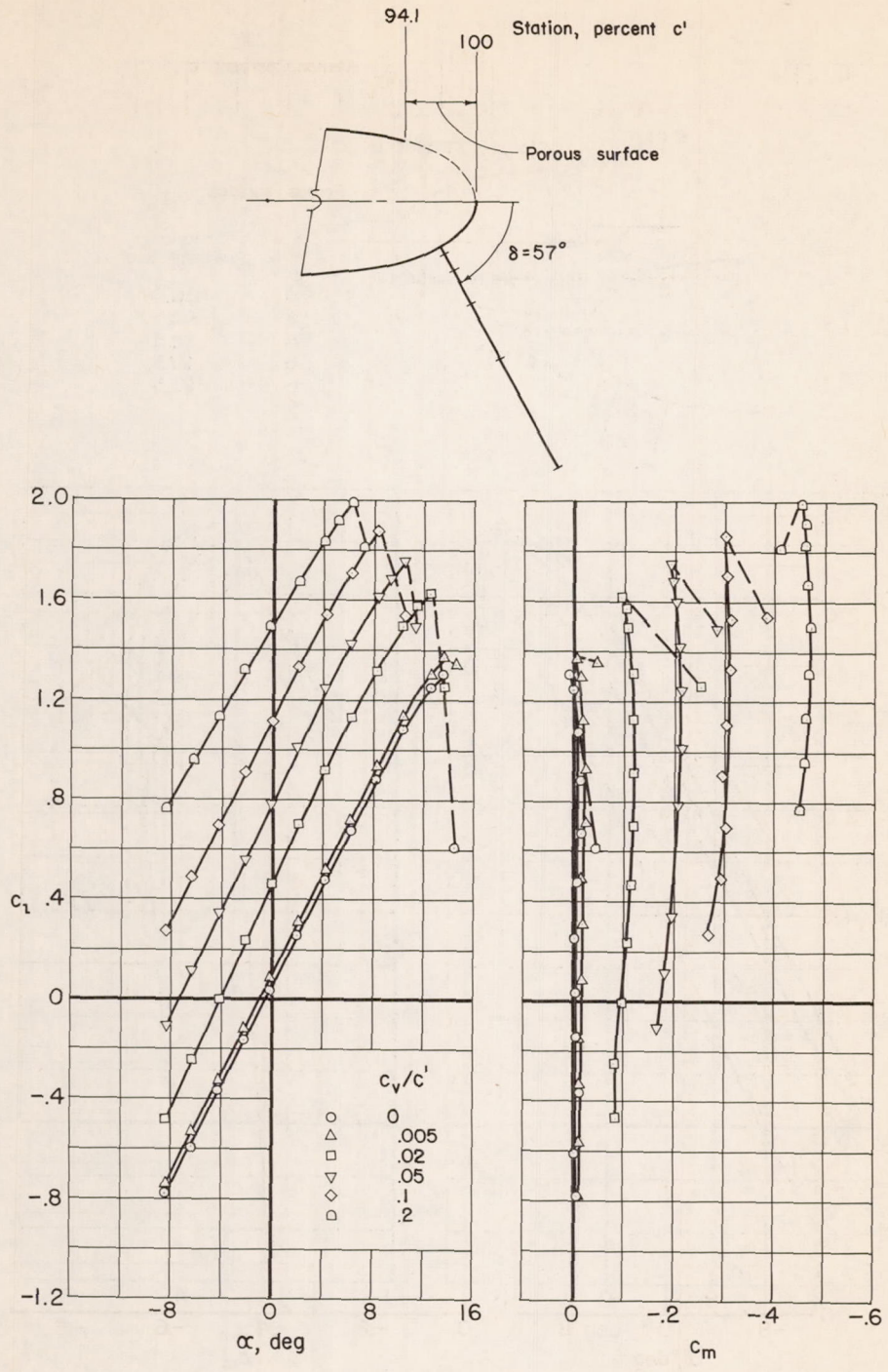

(a) $c_Q = 0$

Figure 14.- Section lift and pitching-moment coefficients for the model with various chord vanes; porous area from 0.941c' on upper surface to trailing edge; $\delta = 57^\circ$.

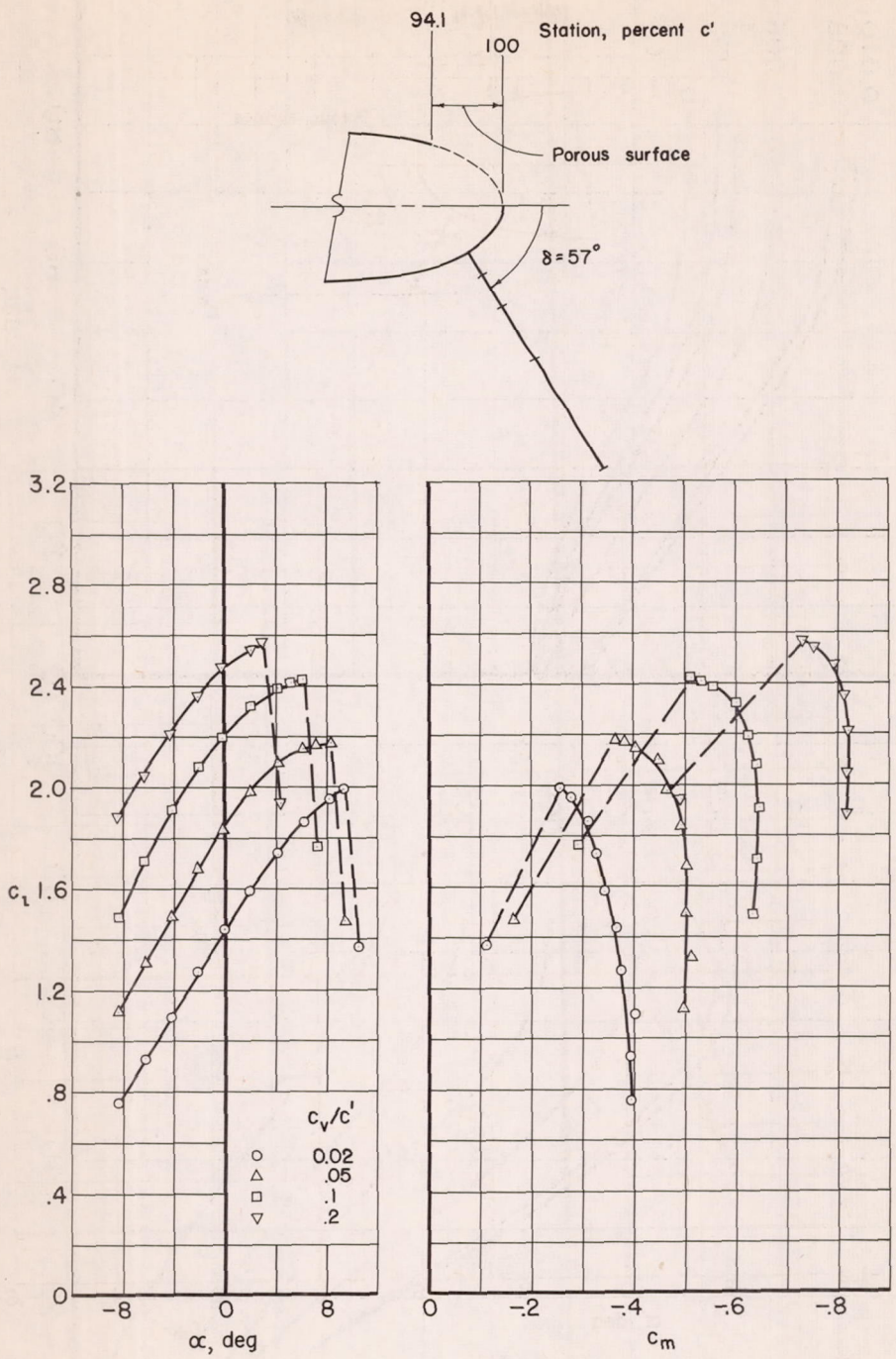

(b) $c_Q = 0.010$

Figure 14.- Concluded.

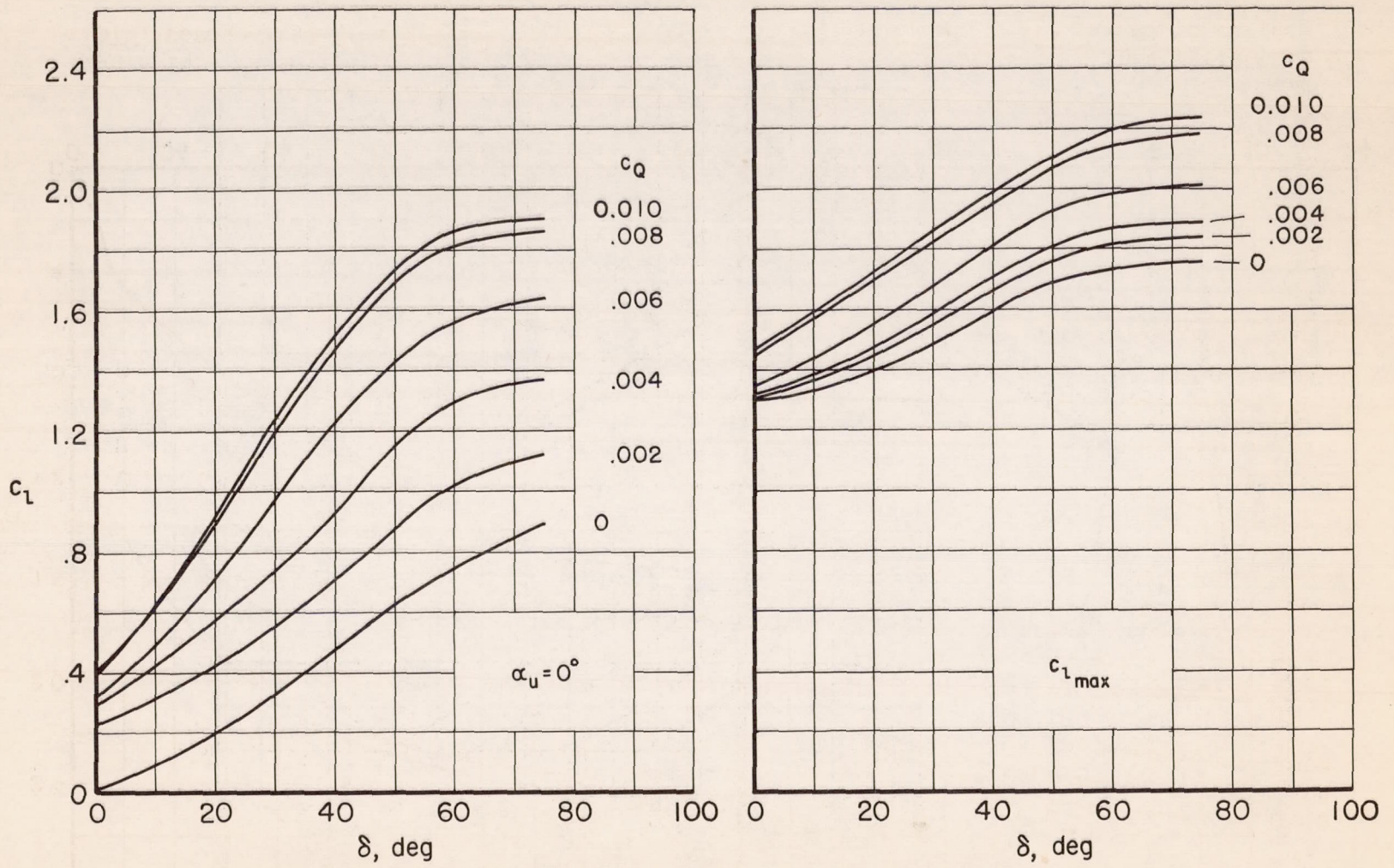

Figure 15.- Variation of section lift coefficient with vane deflection for the model with 0.05c' vane; porous area from 0.941c' on upper surface to trailing edge; vane normal to surface.

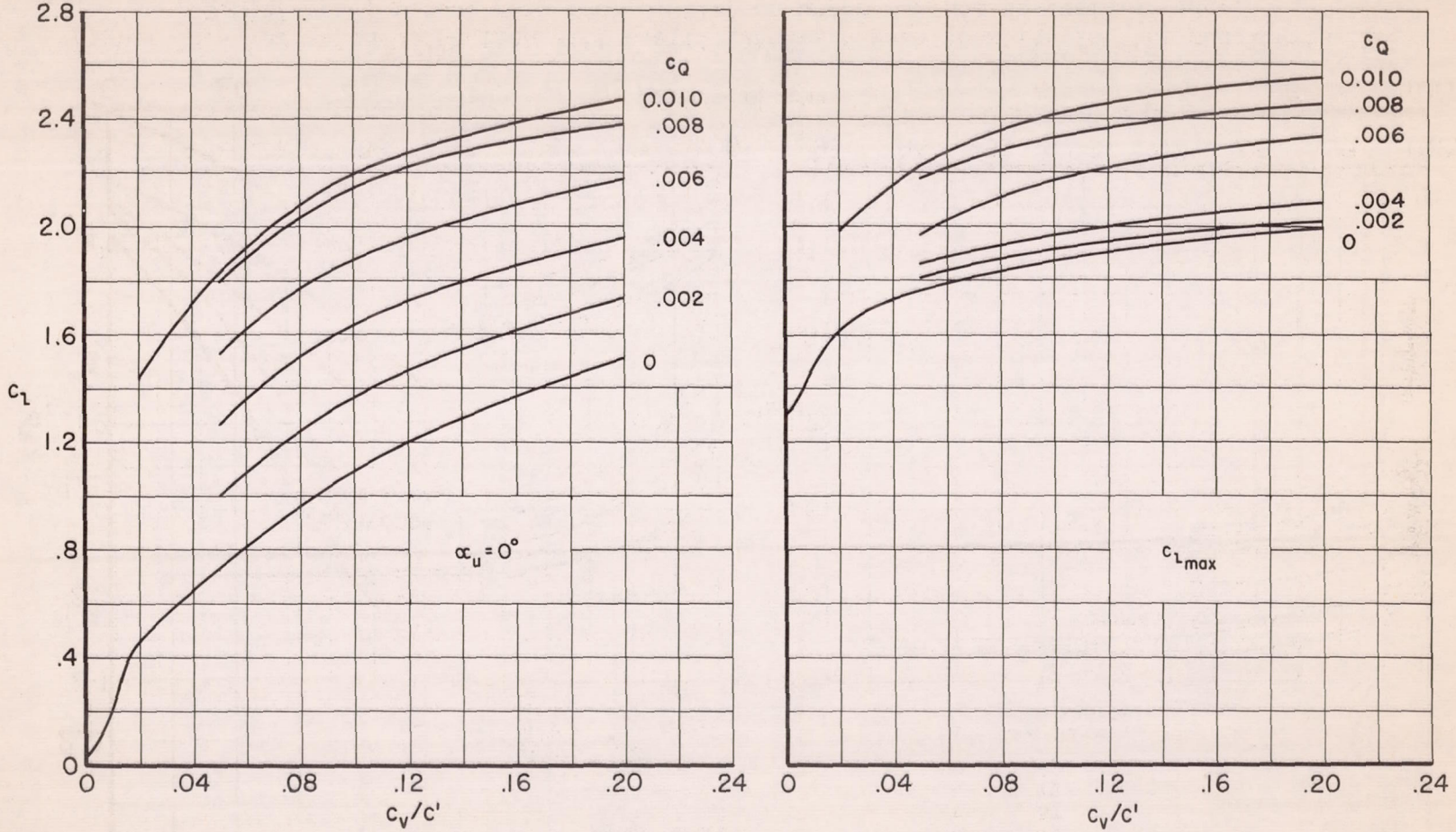

Figure 16.- Variation of section lift with vane chord for the model with a vane deflection of 57°; porous area from 0.941c' on upper surface to trailing edge; vanes normal to surface.

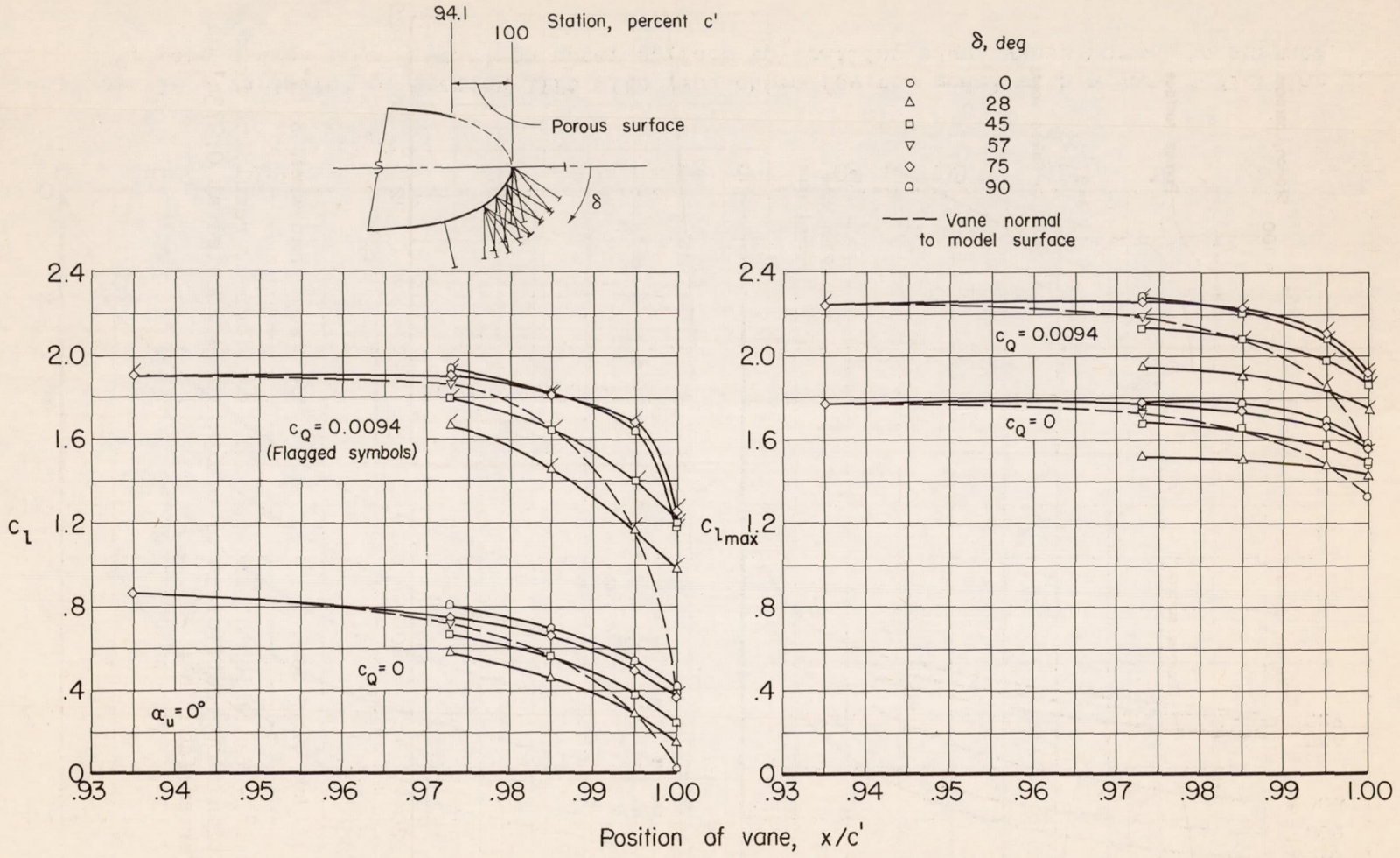

Figure 17.- Variation of section lift coefficient with vane location for the model with the 0.05c' vane; porous area from 0.941c' on upper surface to trailing edge.

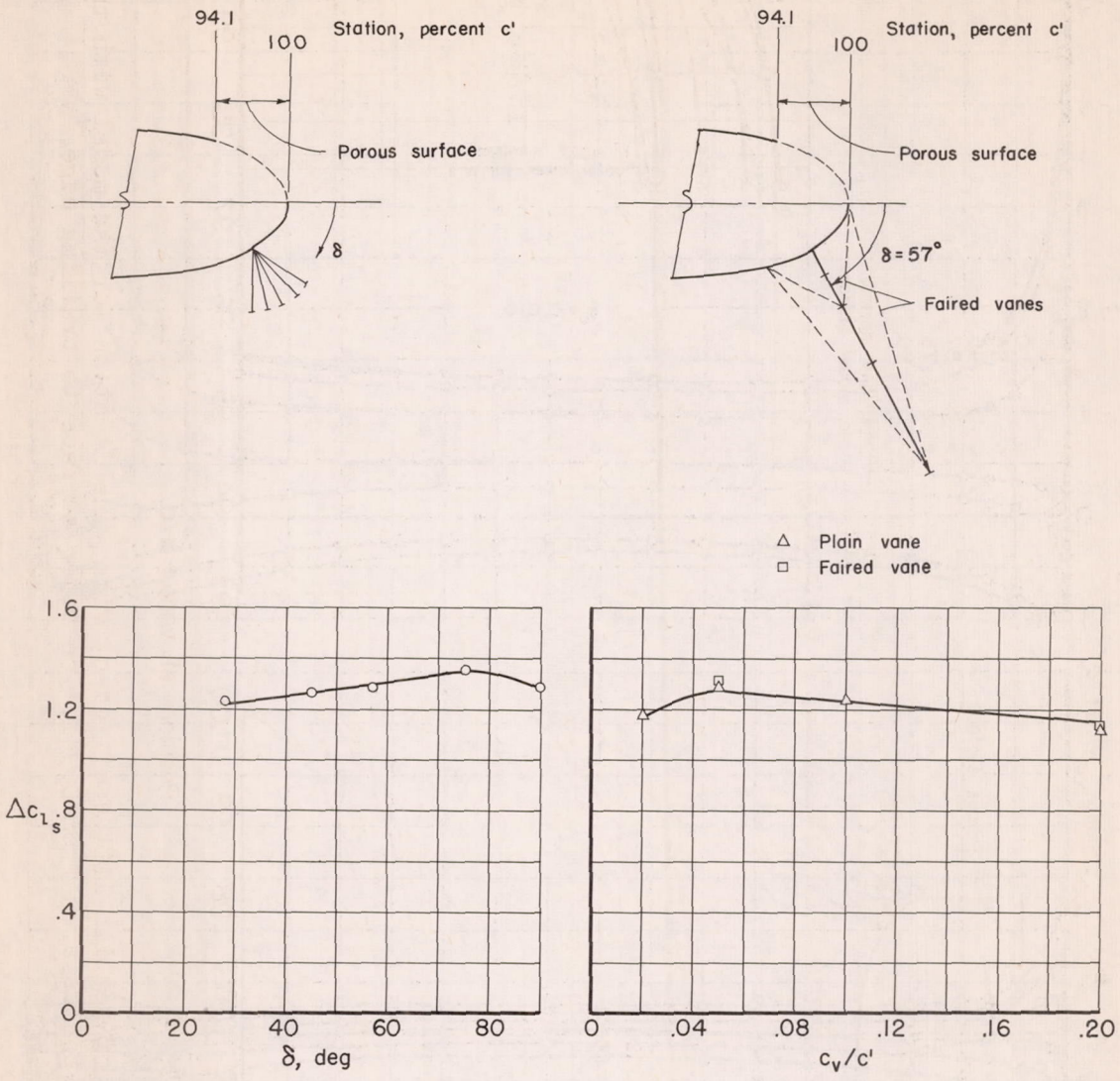

(a) 0.05c' vane.

(b) Various chord vanes, δ = 57°.

Figure 18.- Variation of section lift coefficient resulting from a section flow coefficient of 0.010; vanes located at 0.973c' on lower surface; $\alpha = -8^{\circ}$.

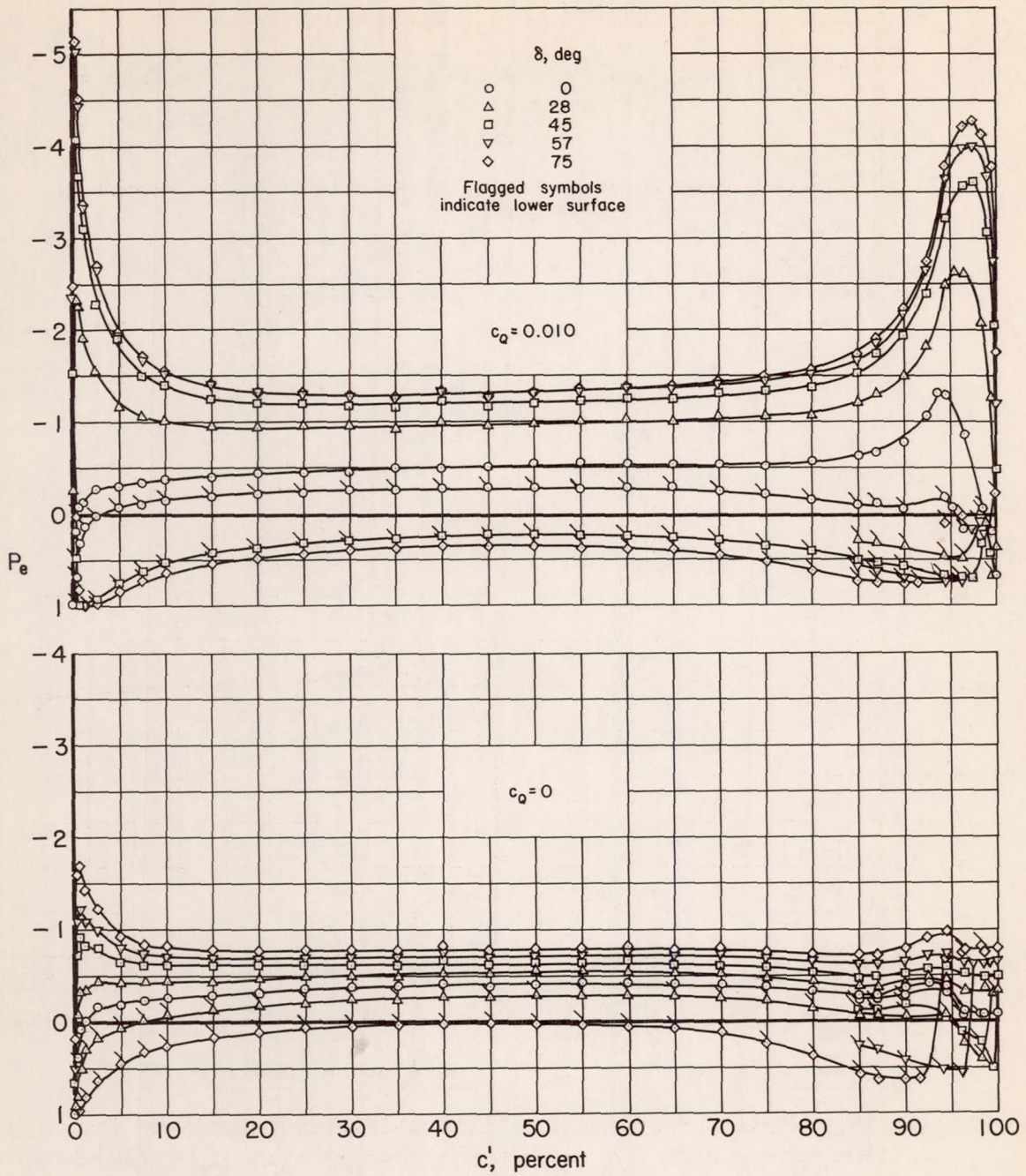

(a) 0.05c' vane normal to surface.

Figure 19.- Chordwise distribution of pressure; porous area from 0.941c' on upper surface to trailing edge; $\alpha = 0^\circ$.

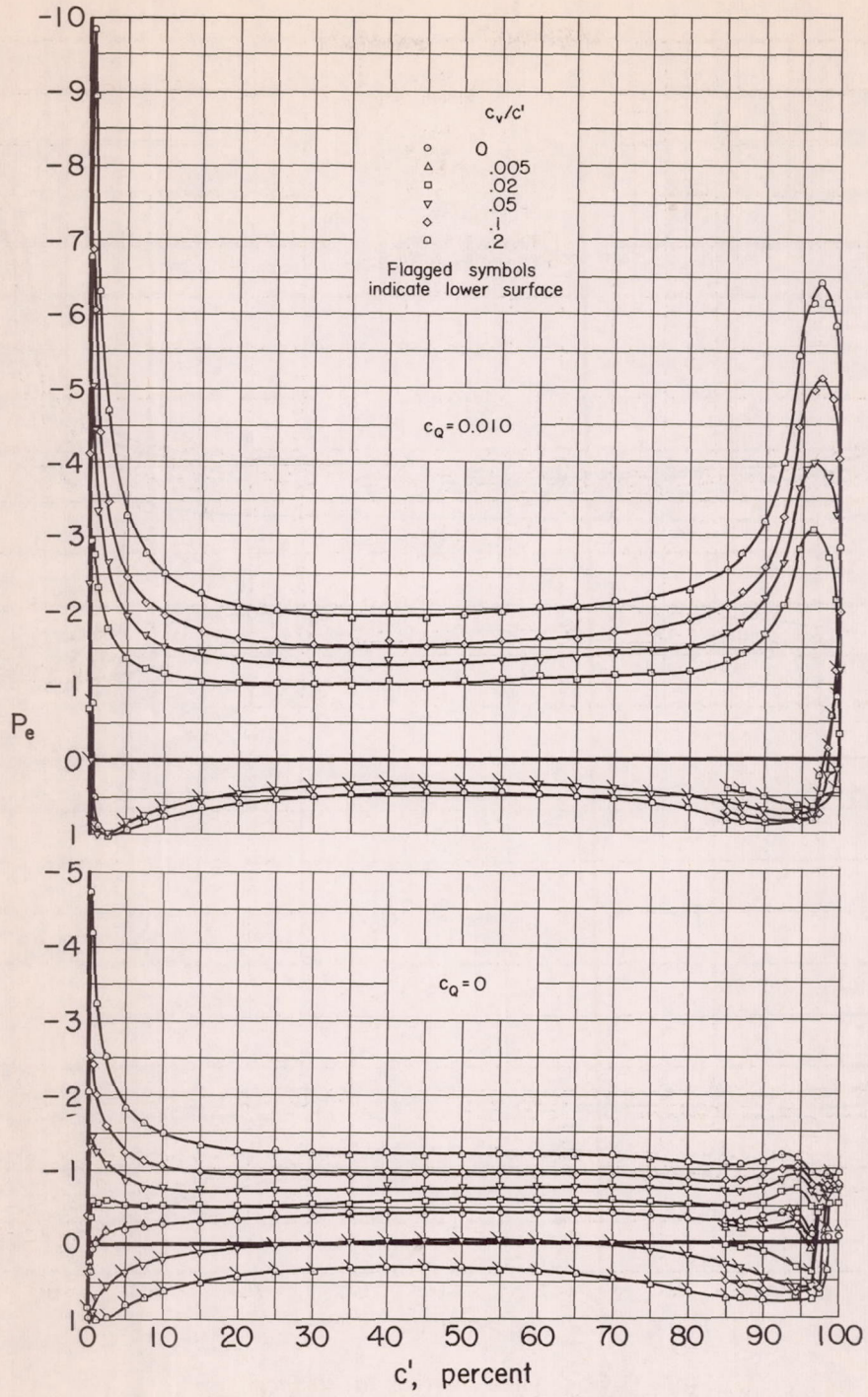

(b) Various chord vanes normal to surface, $\delta = 57°$.

Figure 19.- Continued.

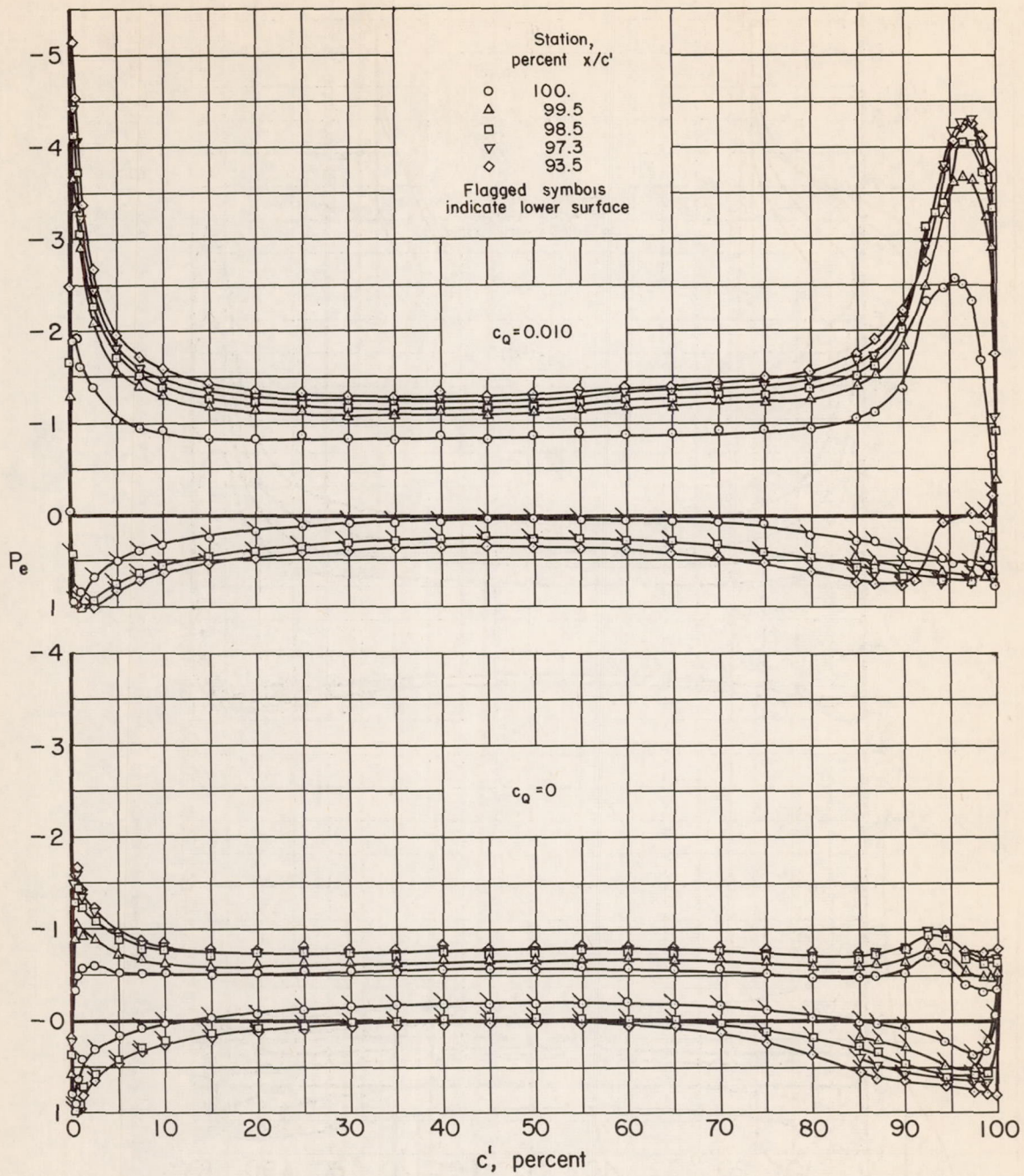

(c) 0.05c' vane at various chordwise stations; $\delta = 75°$.

Figure 19.- Concluded.

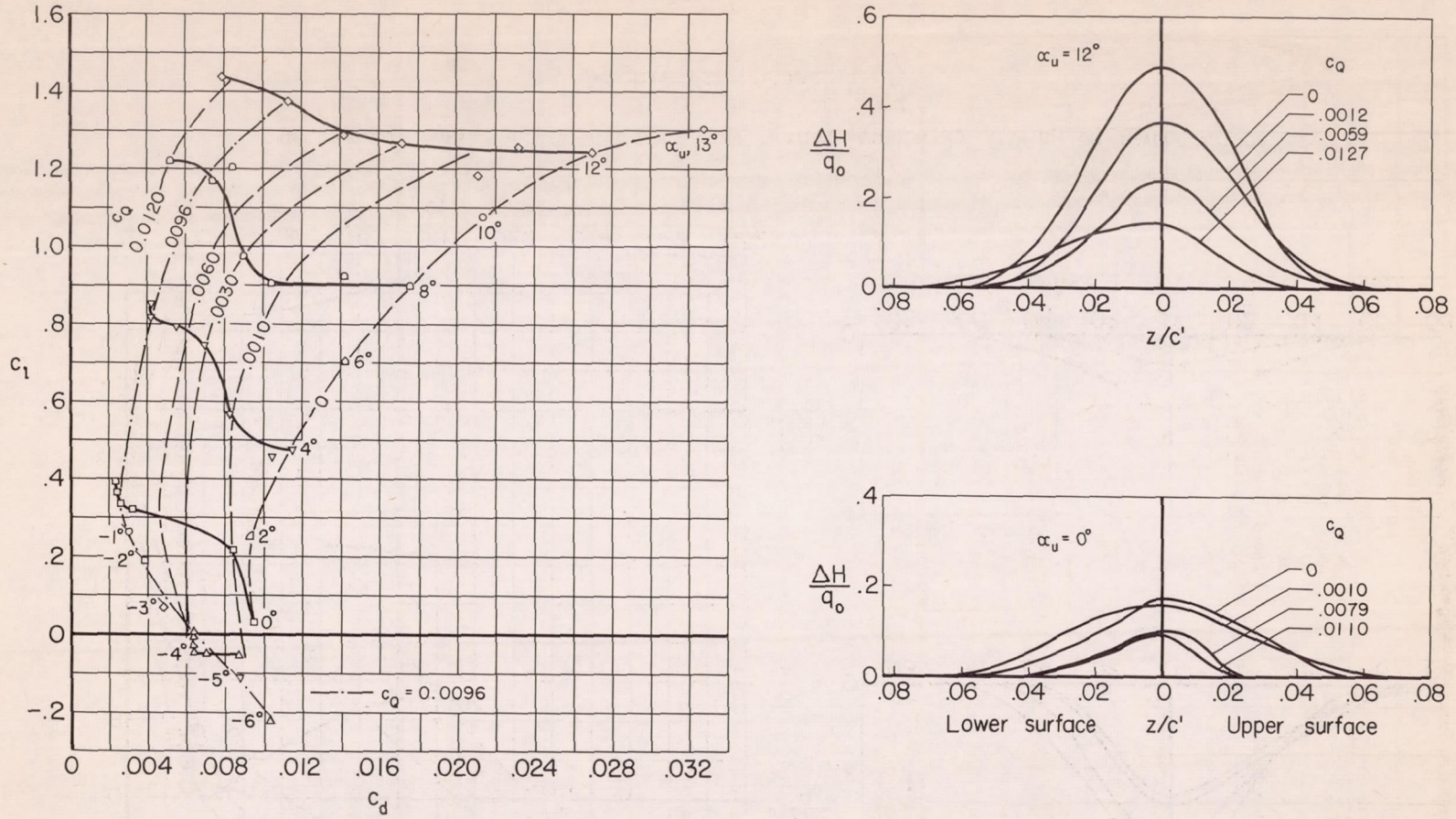

(a) Porous area from 0.89c' on upper surface to trailing edge.

Figure 20.- Wake drag and total-pressure loss in the wake for the model with the 0.05c' vane; $\delta = 0^o$.

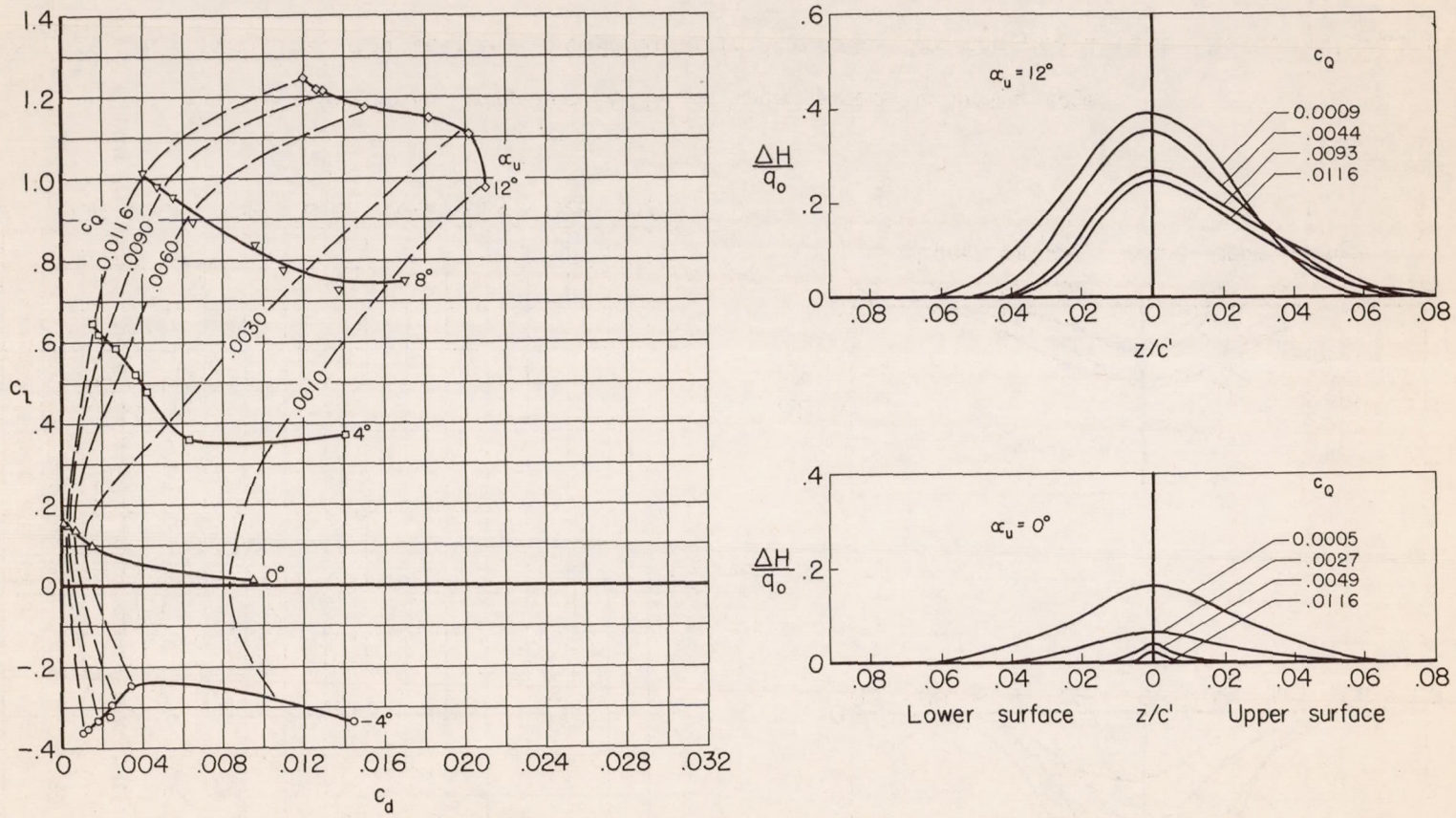

(b) Porous area from 0.941c' on upper surface around to 0.941c' on lower surface.

Figure 20.- Concluded.

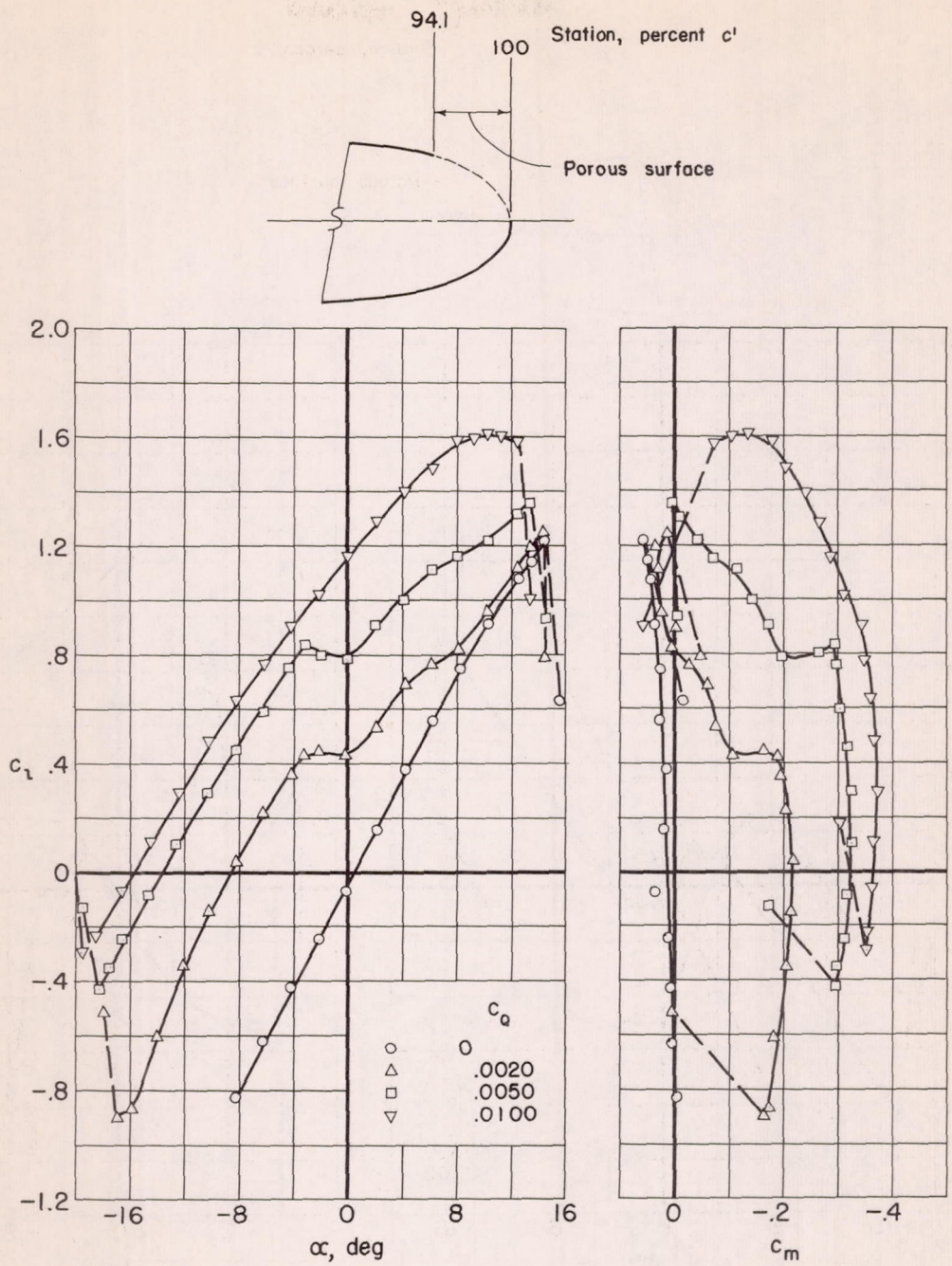

(a) Porous area from 0.941c' on upper surface to trailing edge.

Figure 21.- Section lift and pitching-moment coefficients for the model with the vane removed.

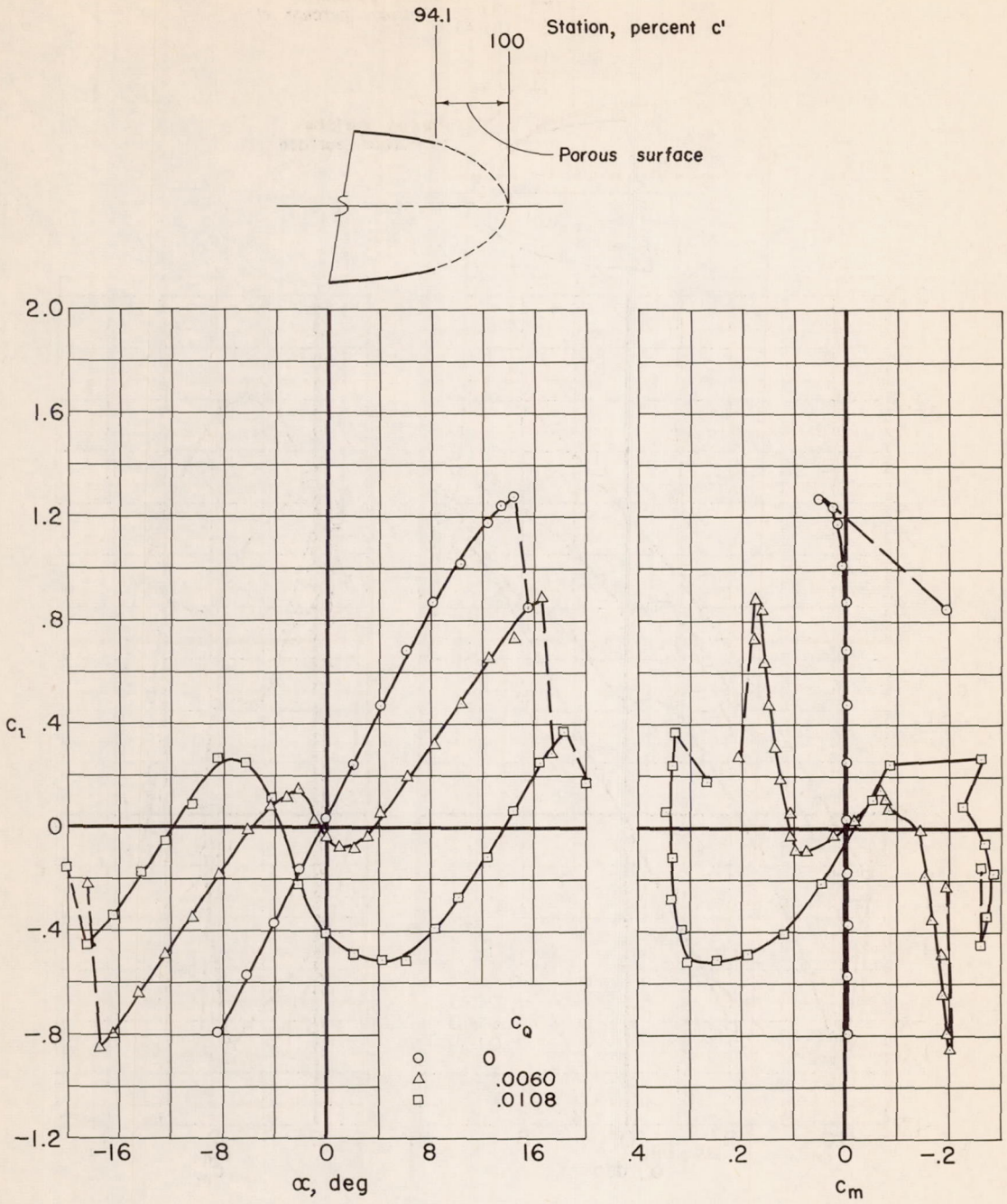

(b) Porous area from 0.941c' on upper surface around to 0.941c' on lower surface.

Figure 21.- Continued.

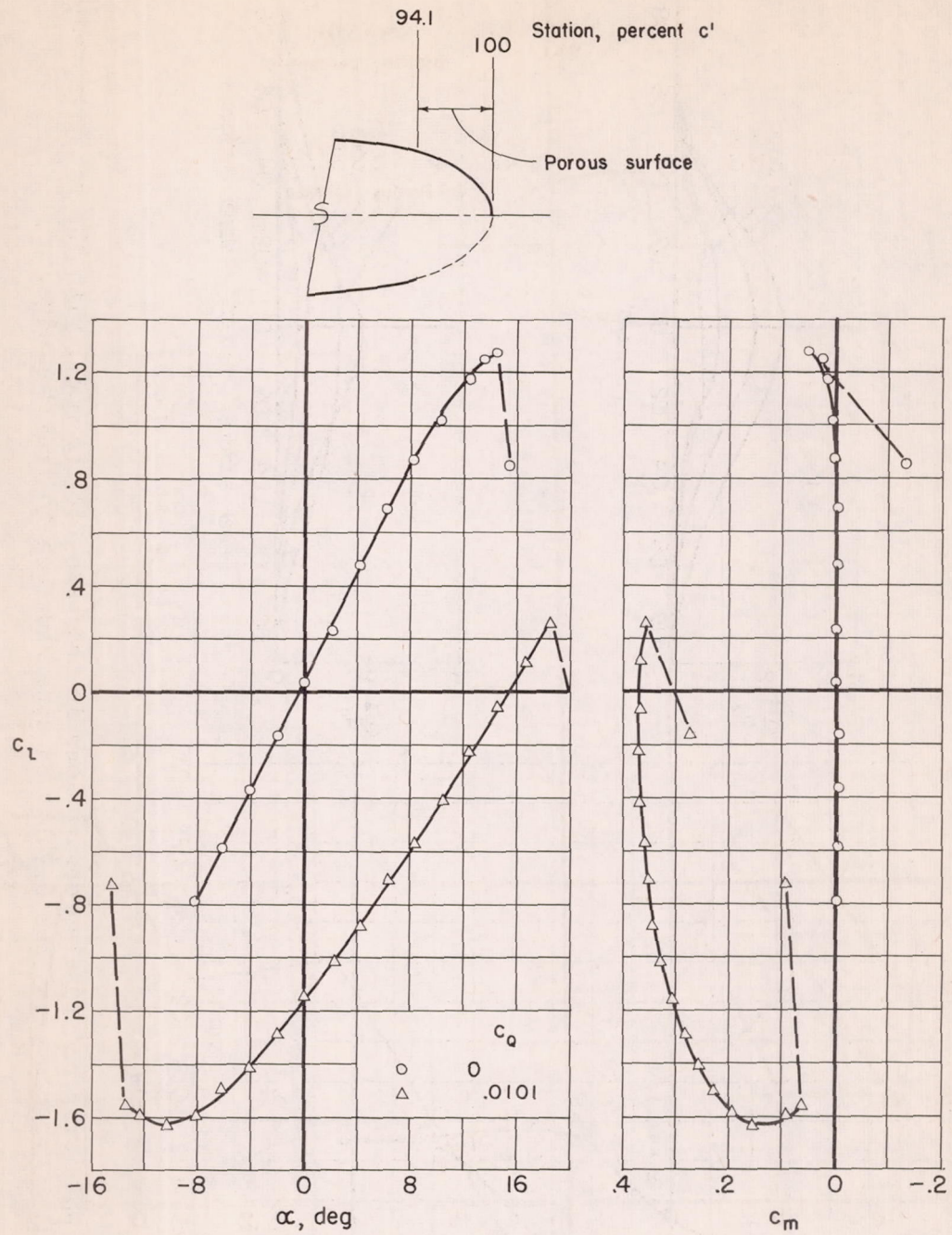

(c) Porous area from 0.94lc' on lower surface to trailing edge.

Figure 21.- Concluded.

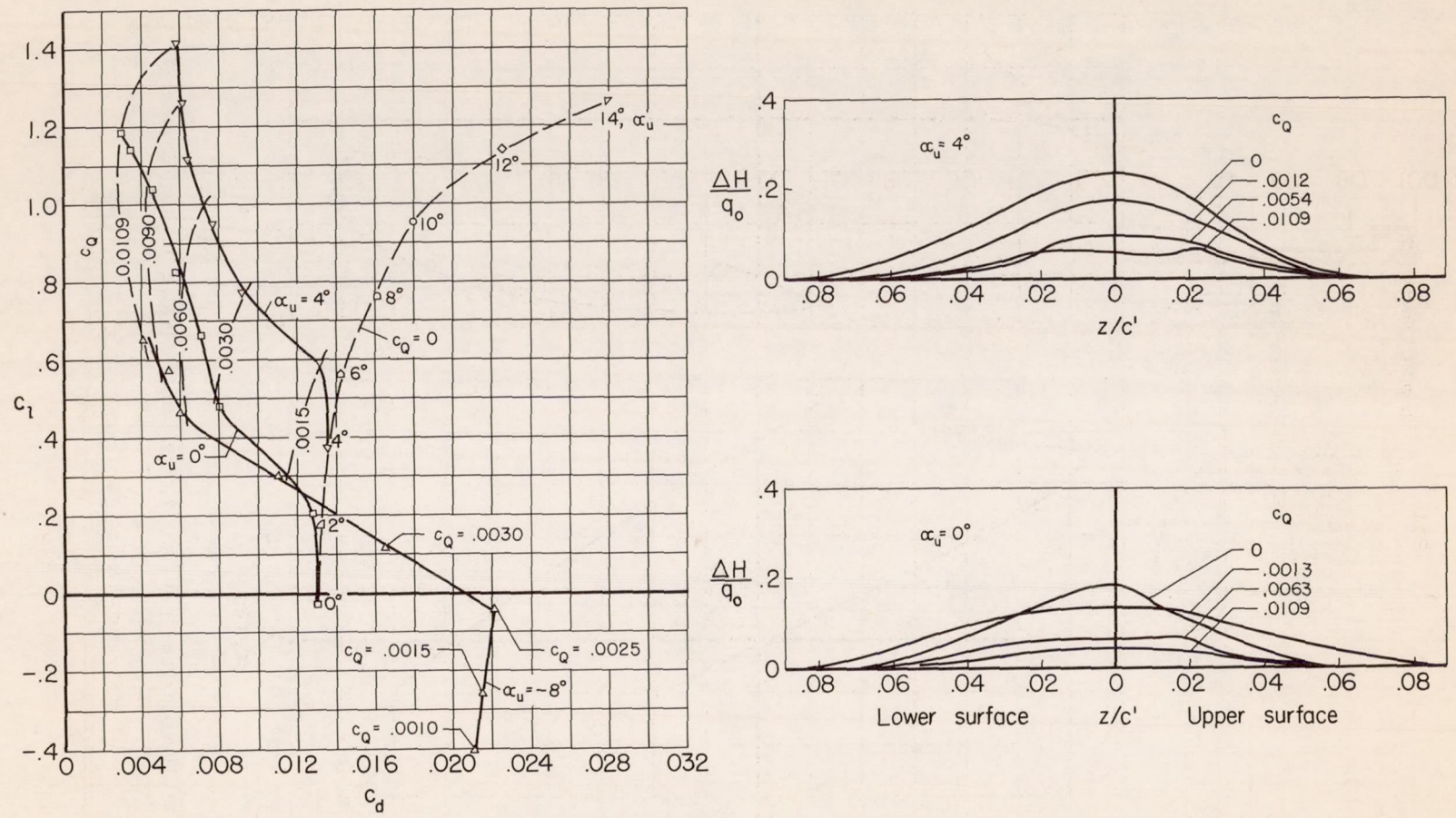

Figure 22.- Wake drag and total-pressure loss in the wake for the model with the vane removed; porous area from 0.941c' on upper surface to trailing edge.

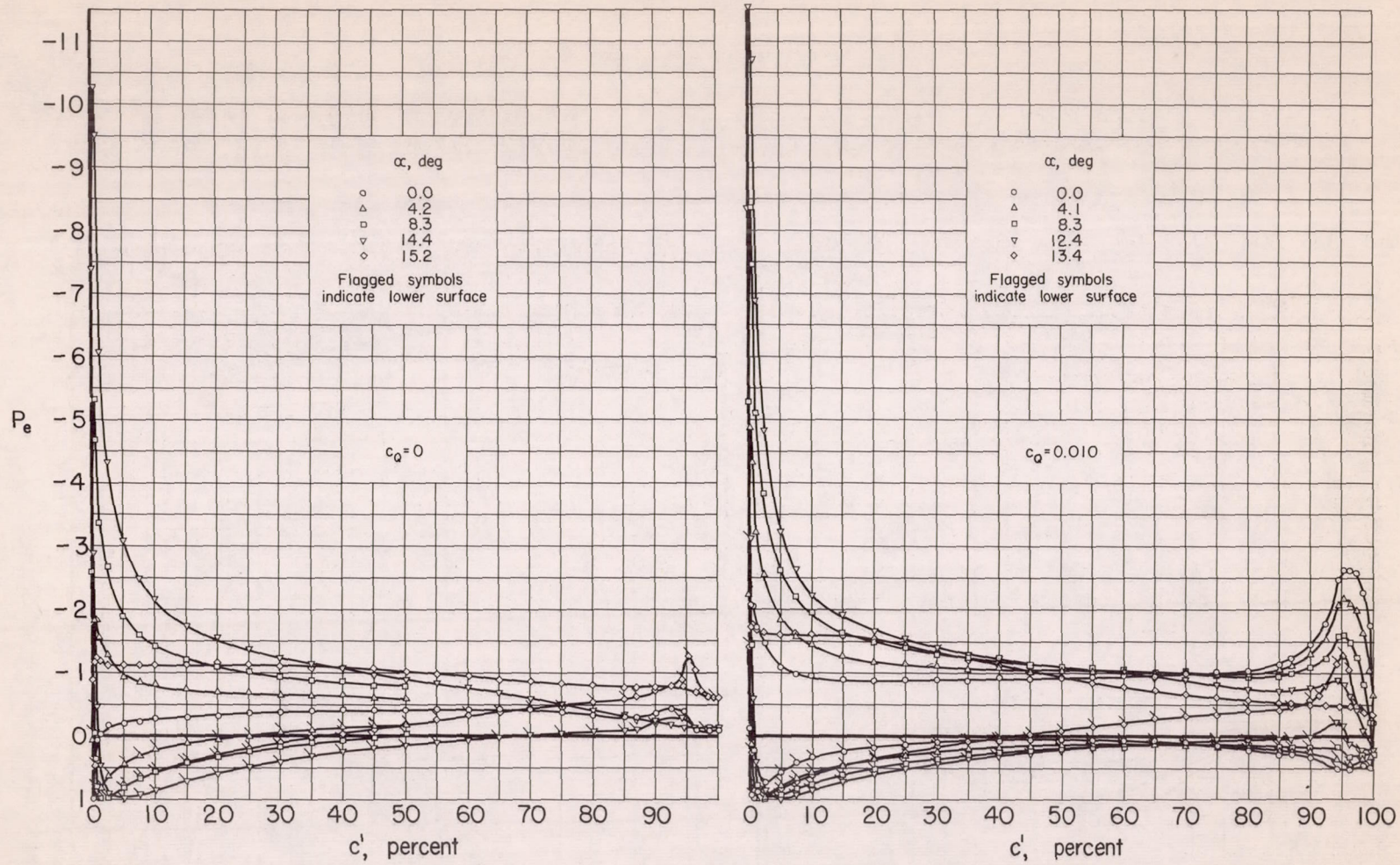

(a) Porous area from 0.94lc' on upper surface to trailing edge.

Figure 23.- Chordwise distribution of pressure for the model with the vane removed.

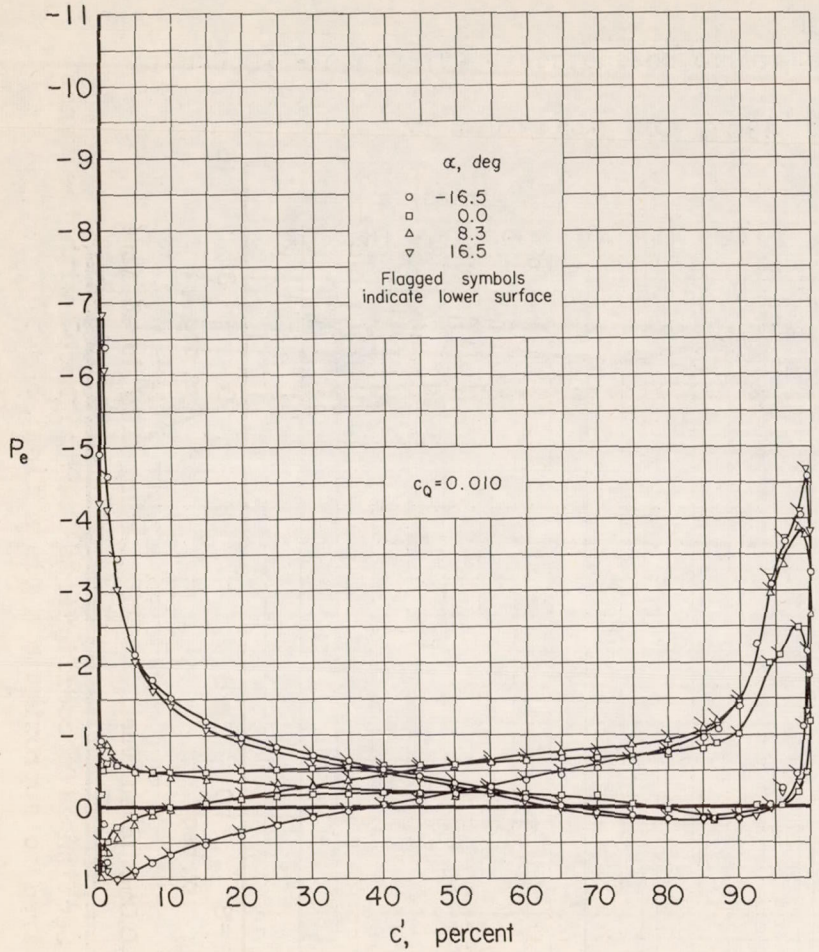

(b) Porous area from 0.941c' on upper surface around to 0.941c' on lower surface.

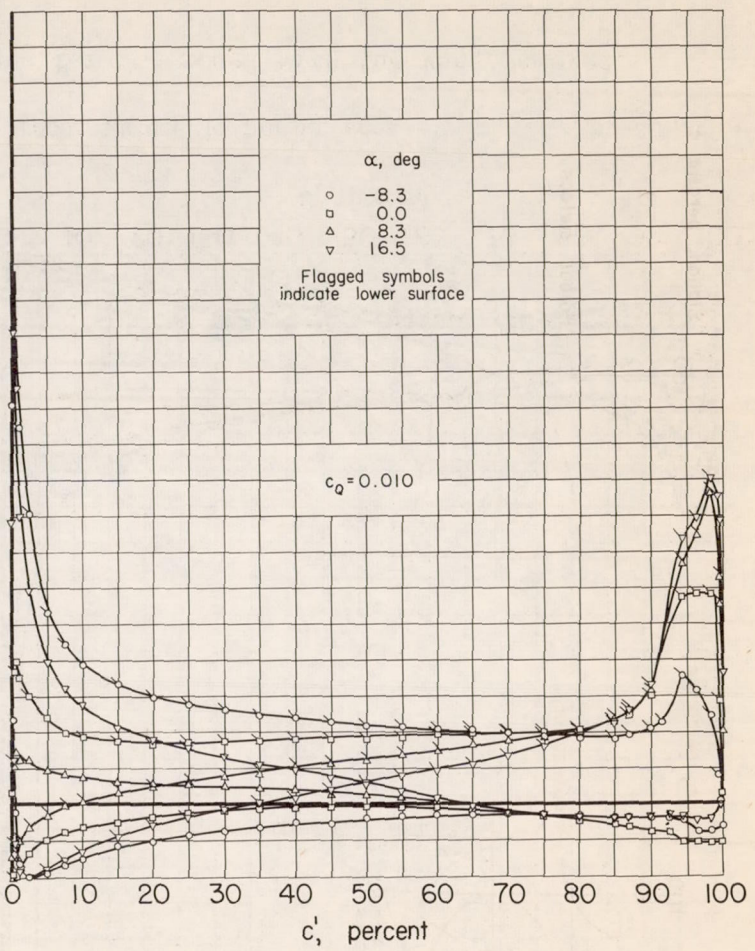

(c) Porous area from 0.941c' on lower surface to trailing edge.

Figure 23.- Concluded.

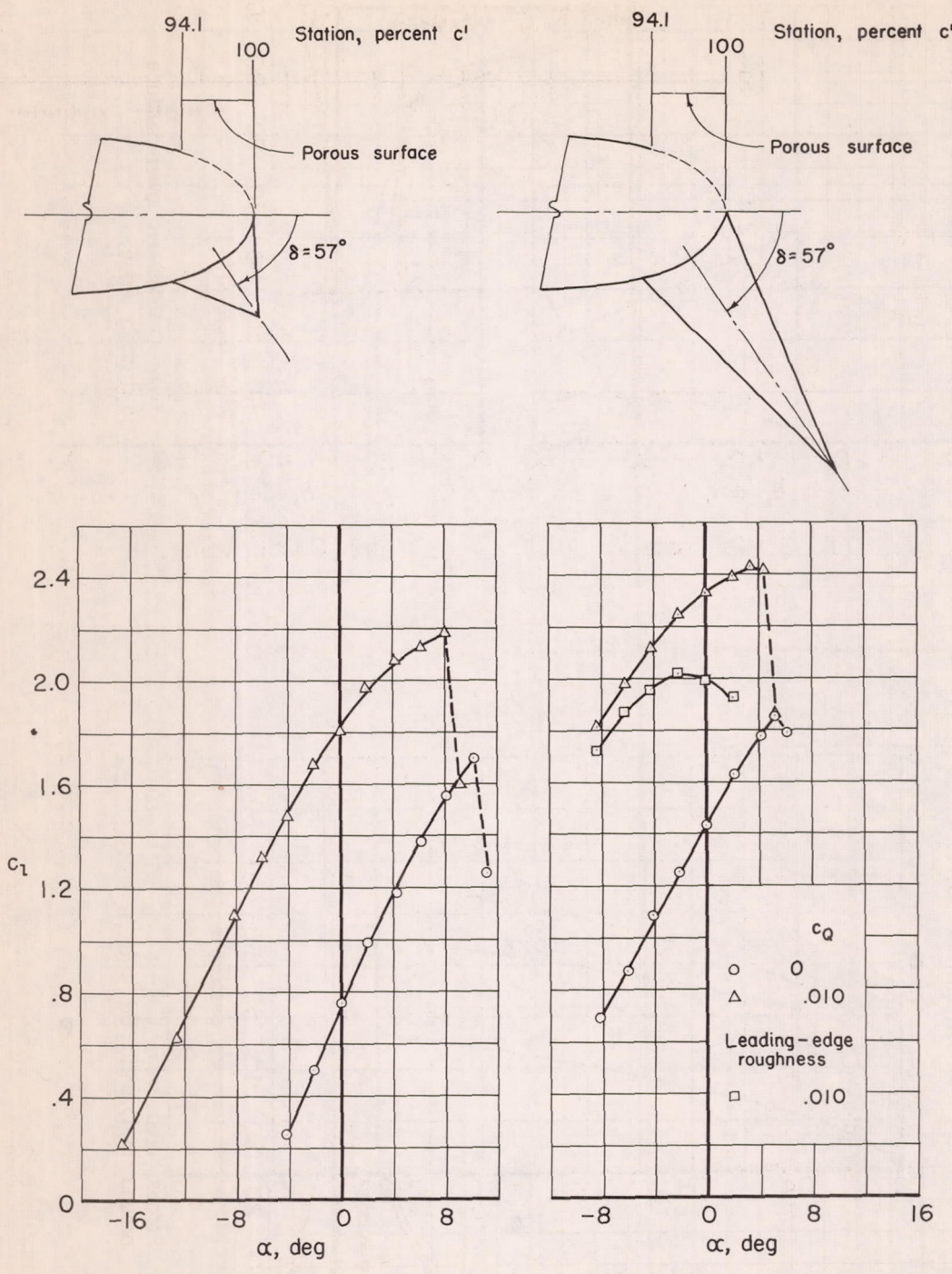

(a) 0.05c' faired vane. (b) 0.2c' faired vane.

Figure 24.- Section lift coefficients for the model with the vanes faired to approximate a plain flap; $\delta = 57^\circ$.

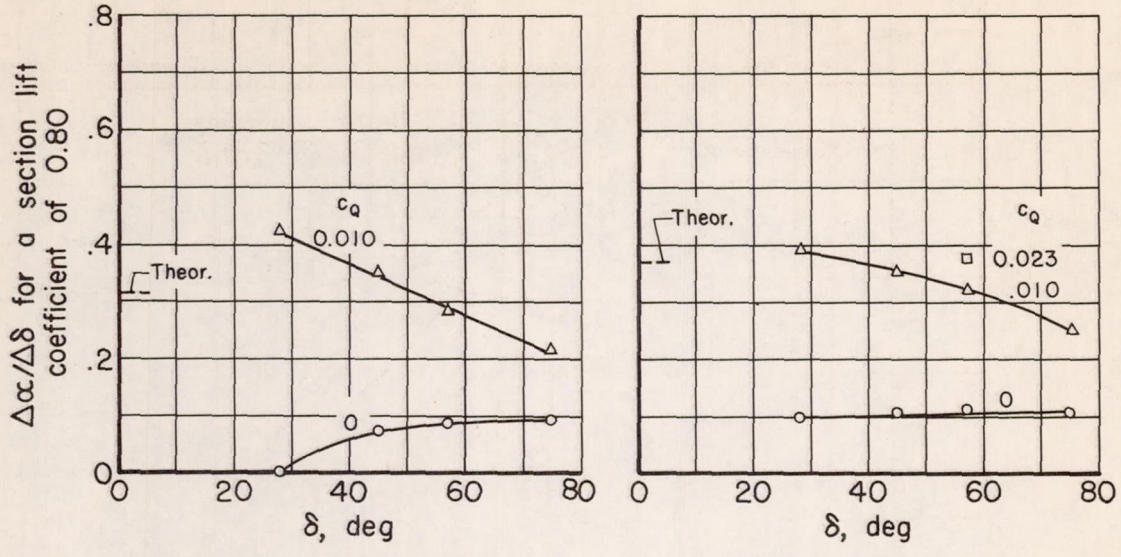

(a) 0.02c' vane. (b) 0.05c' vane.

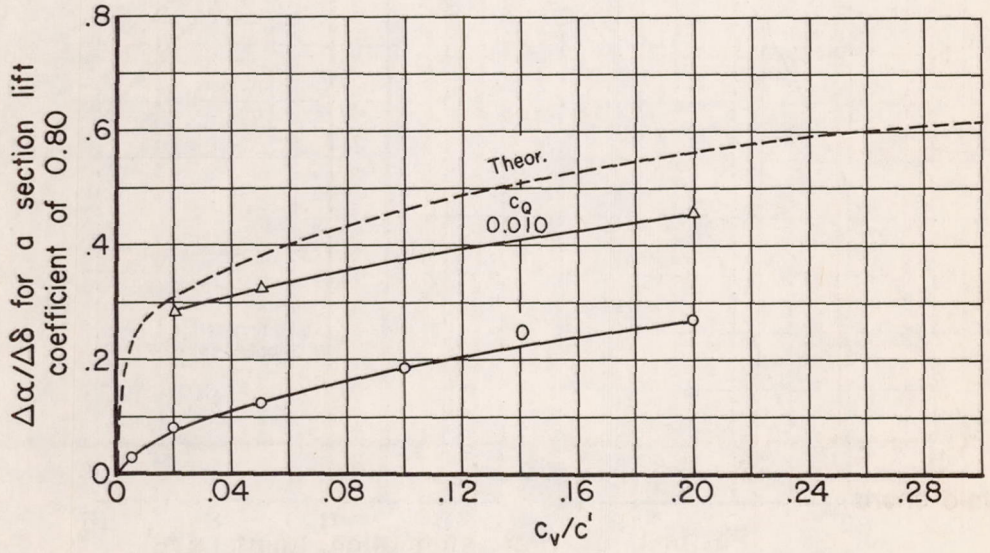

(c) Various chord vanes; δ=57°.

Figure 25.- Control-surface characteristics of the model with various vane arrangements.

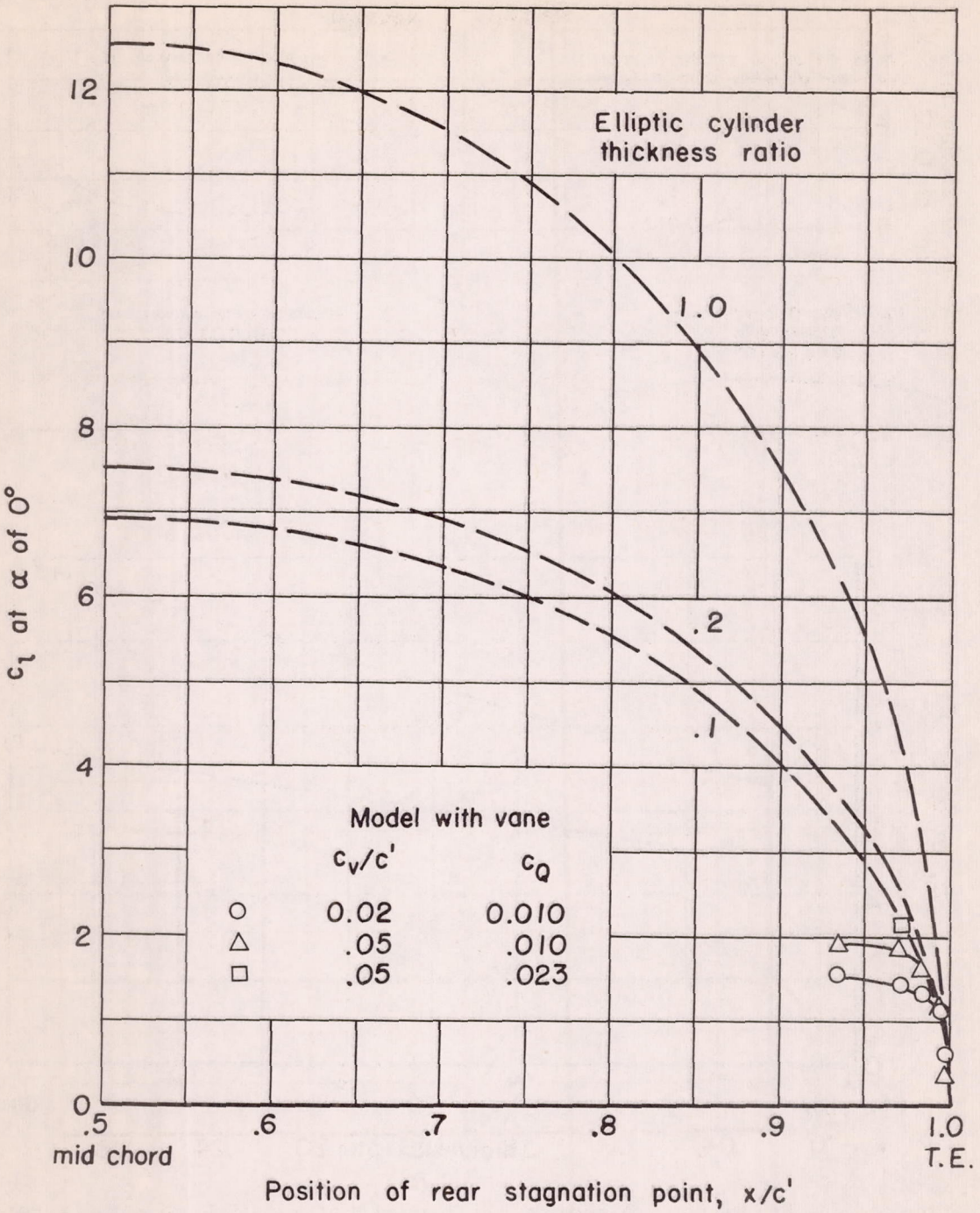

Figure 26.- Calculated variation of section lift coefficient for an elliptic cylinder in potential flow with position of the rear stagnation point, and the variation of section lift coefficient for the model with vane position; $\alpha = 0^\circ$.

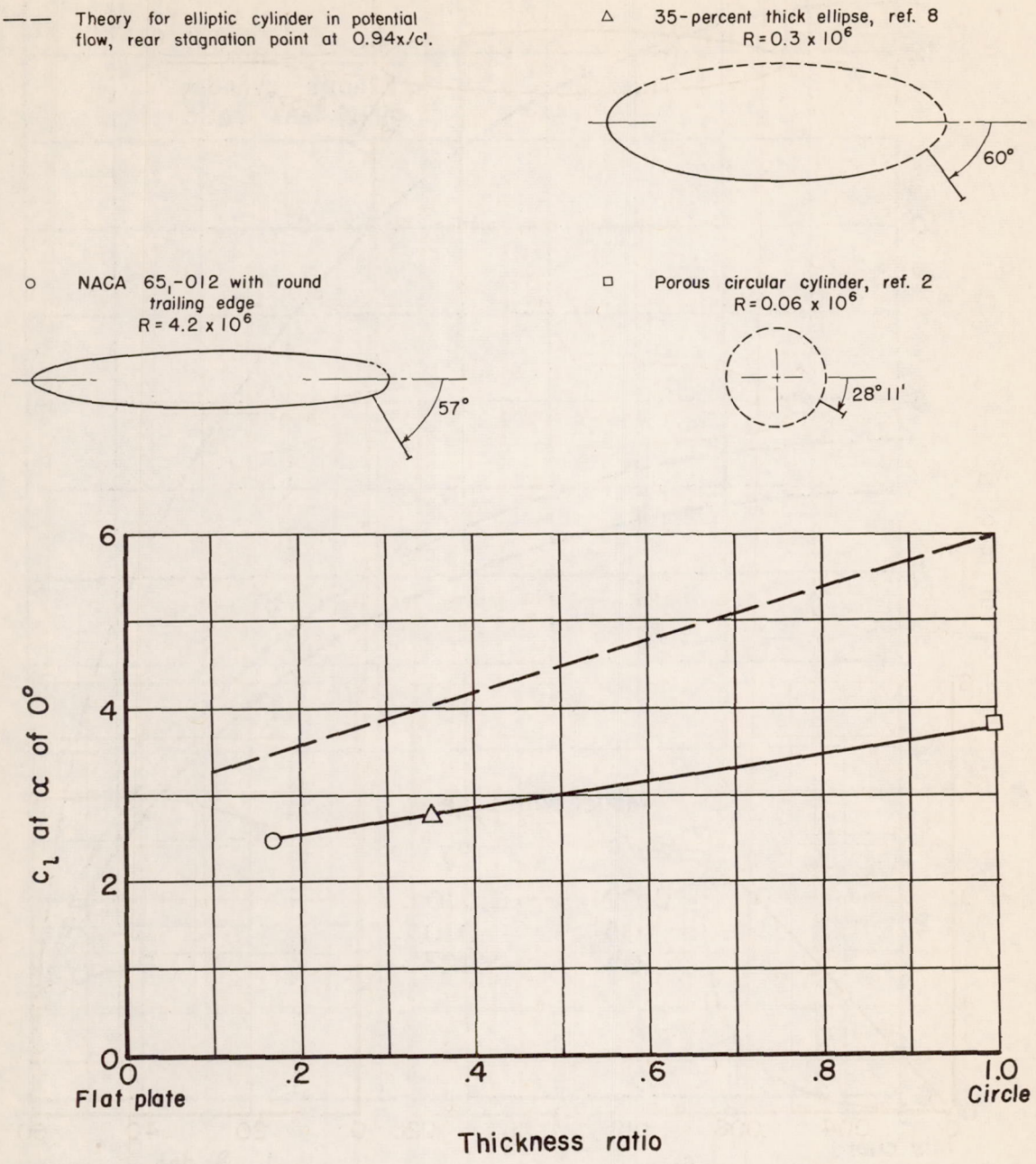

Figure 27.- Variation of section lift coefficient with thickness ratio for profiles with porous, round trailing edges and control vanes; $c_v/c' = 0.2$; $\alpha_u = 0^\circ$; leading edges of vanes at 0.94 x/c'; vanes normal to surface; c_Q = separation-point c_Q.

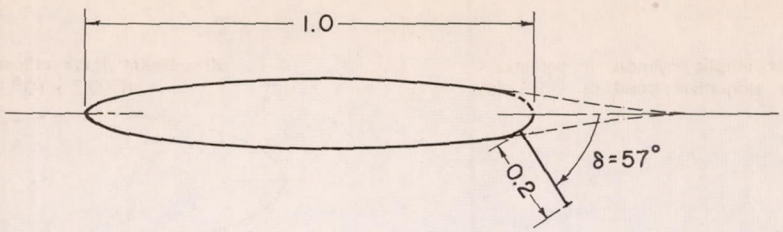

○ Model with area suction, $R = 4.2 \times 10^6$

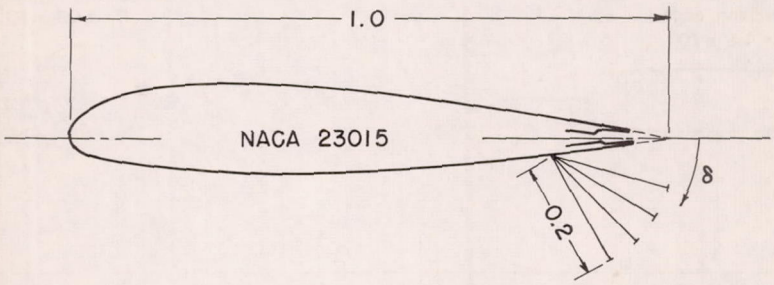

△ Model with slot suction, $R = 0.8 \times 10^6$
(Data from ref. 9)

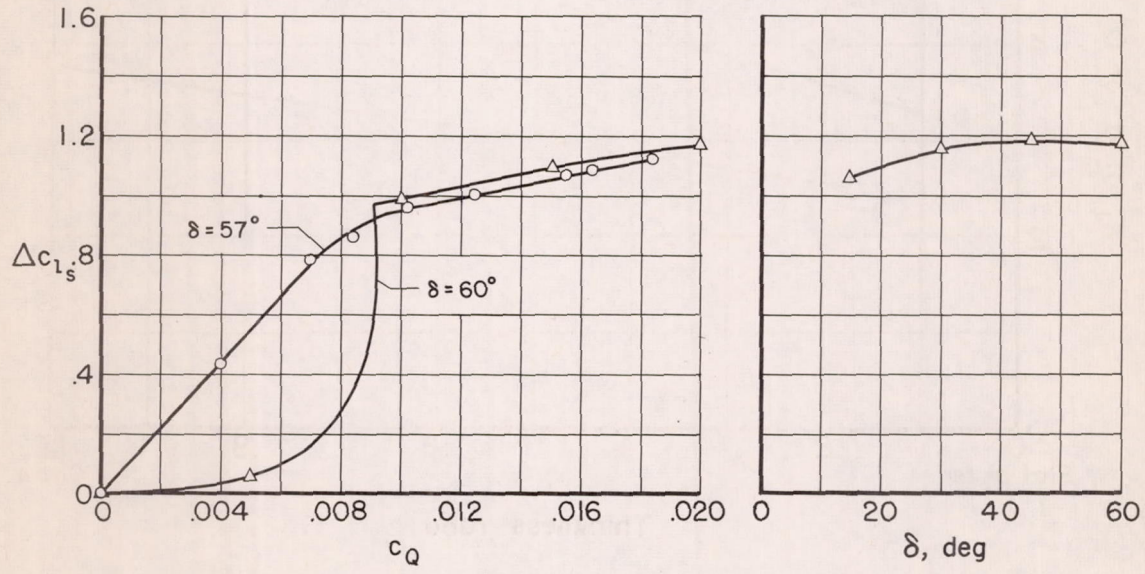

(a) $\alpha = 0°$ (b) $c_Q = 0.020$; $\alpha = 0°$

Figure 28.- Increment of section lift coefficient resulting from suction at the trailing edge.